catalysts

MDPI

Review

Heterogeneous Catalysts for Carbon Dioxide Methanation: A View on Catalytic Performance

Mazhar Ahmed Memon [1], Yanan Jiang [1], Muhammad Azher Hassan [2], Muhammad Ajmal [1], Hong Wang [3,*] and Yuan Liu [1,*]

[1] School of Chemical Engineering, Tianjin University, Tianjin 300350, China; mazharahmed@tju.edu.cn (M.A.M.); jyn364@tju.edu.cn (Y.J.); engrajmal948@gmail.com (M.A.)
[2] Tianjin Key Laboratory of Indoor Air Environmental Quality Control, School of Environment Science & Engineering, Tianjin University, Tianjin 300072, China; azher@tju.edu.cn
[3] Chemical Engineering College, Inner Mongolia University of Technology, Hohhot 010051, China
* Correspondence: hongwang396@imut.edu.cn (H.W.); yuanliu@tju.edu.cn (Y.L.)

Abstract: CO_2 methanation offers a promising route for converting CO_2 into valuable chemicals and energy fuels at the same time as hydrogen is stored in methane, so the development of suitable catalysts is crucial. In this review, the performance of catalysts for CO_2 methanation is presented and discussed, including noble metal-based catalysts and non-noble metal-based catalysts. Among the noble metal-based catalysts (Ru, Rh, and Pd), Ru-based catalysts show the best catalytic performance. In the non-noble metal catalysts, Ni-based catalysts are the best among Ni-, Co-, and Fe-based catalysts. The factors predominantly affecting catalytic performance are the dispersion of the active metal; the synergy of the active metal with support; and the addition of dopants. Further comprehensive investigations into (i) catalytic performance under industrial conditions, (ii) stability over a much longer period and (iii) activity enhancement at low reaction temperatures are anticipated to meet the industrial applications of CO_2 methanation.

Keywords: carbon dioxide; methanation; hydrogen; heterogeneous catalyst; nickel; ruthenium; carbon neutrality

Citation: Memon, M.A.; Jiang, Y.; Hassan, M.A.; Ajmal, M.; Wang, H.; Liu, Y. Heterogeneous Catalysts for Carbon Dioxide Methanation: A View on Catalytic Performance. *Catalysts* **2023**, *13*, 1514. https://doi.org/10.3390/catal13121514

Academic Editor: Enrique García-Bordejé

Received: 7 November 2023
Revised: 10 December 2023
Accepted: 12 December 2023
Published: 15 December 2023

1. Introduction

Fossil fuels have been considered the world's principal energy resource since the early 1970s [1–3]. After the industrial revolution, using different energy sources led to global warming and climate change [4,5]. Oil industries, power production plants, cement factories, steel, building constructions, and iron manufacturers are regarded as major contributors to the rise in the emission of carbon dioxide (CO_2), which is a well-known greenhouse gas [6–9]. The sixth report of the Intergovernmental Panel on Climate Change (IPCC) states that global net anthropogenic emissions include a considerable amount of CO_2, equivalent to 75%, which is the byproduct of the world energy sector [10]. Moreover, anthropogenic CO_2 is a promoter of many other pollutants and a predominant global warming precursor [5,11,12]. Fossil fuels, industrial processes, land use change, and forestry are significantly responsible for releasing CO_2 into the environment, as shown in Figure 1a. Region-wise global cumulative net anthropogenic CO_2 is shown in Figure 1b [13]. The cumulative net anthropogenic analysis reveals North America is the lead emitter, releasing 23% of CO_2 into the environment from 1850 to 2019.

CO_2 emissions into the atmosphere are increasing every second, directly affecting global warming and climate change [6,10]. A record increase in CO_2 was reported at 424 parts per million (ppm) on a global average in May 2023, reported by the Mauna Loa Observatory, as shown in Figure 1c. If this ongoing upward trend persists, it could have a detrimental impact on the global average temperature [14]. The recorded average growth in CO_2 concentration in the last decade was 2 ppm per year [15]. The current and projected

trends are identical, as many underdeveloped countries still produce 65% of their energy from the combustion of fossil fuels [16]. It is a harsh reality that we—mankind—are solely responsible for climate change and global warming [3]. Suppose that considerable actions are not taken right now to regulate and stabilize the emission of CO_2 into the atmosphere. In that case, a disastrous threat will come from ecosystem destruction due to heavy rain spells, tornadoes, and storms; flooding from low coastal glaciers melting; and a rise in sea levels [3,10]. Recently, there have been many severe ecological catastrophes in various regions of the globe, including Cyclones Idai and Biparjoy, lethal heatwaves and ambient pollution in the Indo-Gangetic Plain [6] and Europe, and flooding in Southeast Asia. From Mozambique to Bangladesh, millions of people have already lost their homes, livelihoods, and loved ones because of more dangerous and frequent extreme weather events [17].

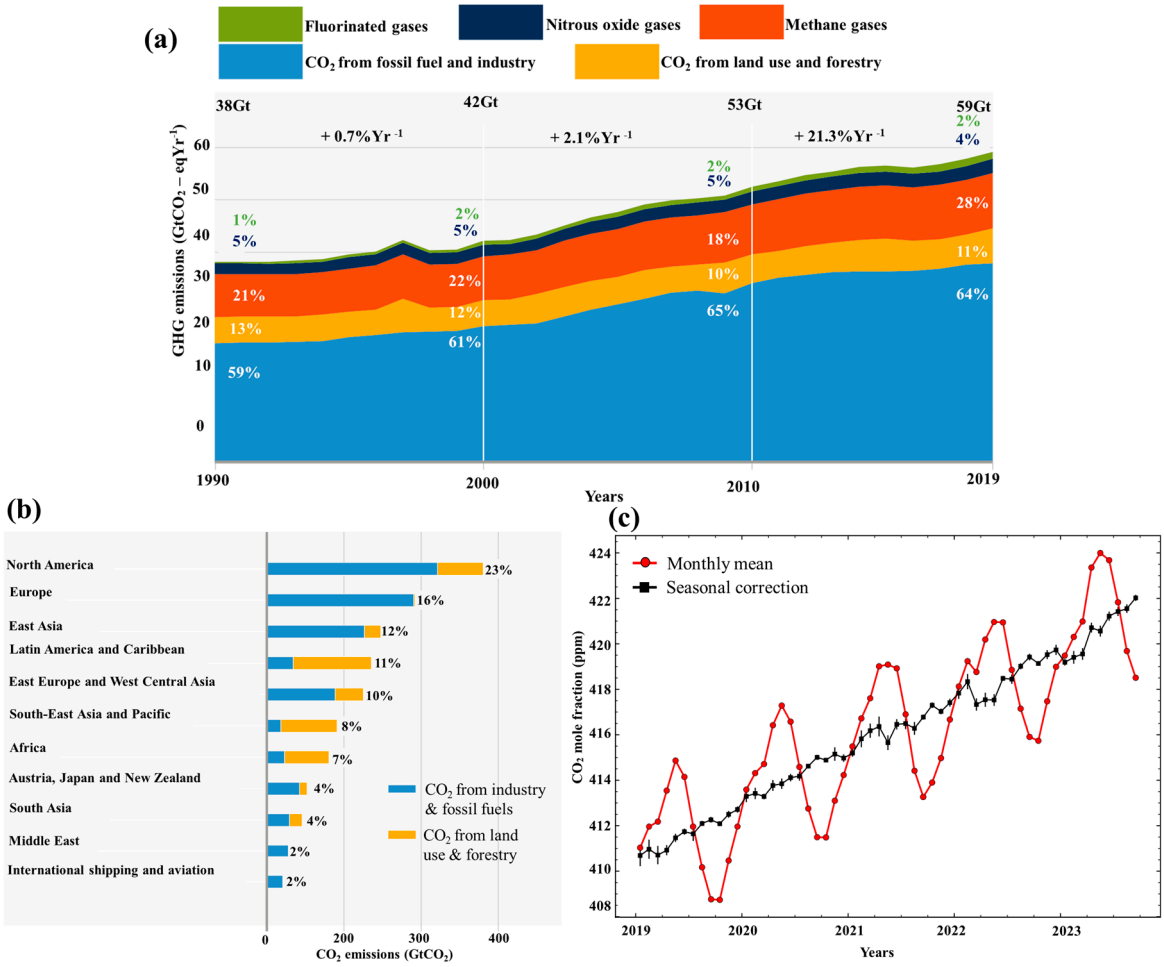

Figure 1. Global trend in CO_2 emissions from 1850 to 2019: (**a**) net anthropogenic emissions [10], (**b**) net anthropogenic emissions per region [13], (**c**) global monthly CO_2 measured by Mauna Loa Observatory [18].

Several international conferences, treaties, and summits have been held to propose a solution to mitigate this situation, such as the 1997 International Agreement on Climate Change and the 2005 Kyoto Protocol in collaboration with the UN, which was held to reduce CO_2 emissions [19]. At the UN Climate Change Conference in Paris in 2017, an agreement was reached to limit the global temperature rise to within 2 °C by minimizing CO_2 emissions [20]. In 2019, the Climate Change Action Summit committed to zero carbon emissions by 2050 [21]. In 2021, the G7 Climate Summit and the annual G20 Summit were conducted with the objective of tackling climate change and advancing the pursuit of carbon neutrality.

Numerous strategies have been proposed in the literature to reduce CO_2 emissions and combat climate change [22–26]. There are two prominent available routes: (i) carbon capture, utilization, and storage (CCUS) and (ii) substituting conventional fuels with renewable energy sources. Both routes can be combined by using CO_2 with renewable power sources, i.e., solar and wind to produce fuel [24,27]. Wind and solar energy are intermittent and variable energy sources, posing challenges to long-term storage. However, renewable energy can produce hydrogen via water electrolysis, for which the storage of hydrogen is also a crucial task. Thus, to address these issues effectively and promote environmentally friendly solutions, utilizing CO_2 alongside renewable energy for fuel production, such as methane (CH_4), emerges as a compelling green alternative. Fuel can consist of hydrocarbons and oxygen (O_2)-containing hydrocarbons, among which, CH_4 holds particular significance.

CH_4 can be produced by utilizing CO_2 and hydrogen (H_2) through CO_2 methanation, also known as the Sabatier process, which is an efficient and appropriate procedure for CO_2 utilization [28–30]. The extant natural gas infrastructure may be used for the CH_4 produced from CO_2 methanation. Thus, this strategy has the potential for large-scale deployment. By integrating CO_2 capture, H_2 from renewable energy, and CO_2 methanation, we can make significant strides in reducing CO_2 emissions, transitioning to a low-carbon economy, and mitigating the impacts of climate change [28,31,32].

For the conversion of CO_2 into CH_4, the largest impediment is developing a highly active and stable catalyst suitable for a cost-effective and large-scale industrial chemical process. To the best of our knowledge, there has been no comprehensive review that covers recent advancements in catalytic performance for the catalysts of CO_2 methanation, including activity, selectivity, and stability. Therefore, the primary focus of this review is to address the roadmap of catalytic performance for CO_2 methanation catalysts by tackling the challenges associated with developing industrial catalysts for CO_2 methanation. The first section provides a basis for understanding the CO_2 methanation reaction by explaining the thermodynamic equilibrium and reaction mechanisms. The second and third sections review the catalytic performance of noble and non-noble metal catalysts and factors that influence the catalytic performance.

2. Reaction Mechanism and Thermodynamic Equilibrium

2.1. CO_2 Methanation Reaction

In 1872, renowned scientist Brodie demonstrated the reduction of CO_2 into CH_4 [16]. Paul Sabatier and Jean Baptiste Senderens analyzed the same results using a heterogeneous catalyst in 1902. Later, in 1912, the Nobel Prize was awarded to Sabatier for CO_2 hydrogenation into CH_4 (the Sabatier reaction) with a well-dispersed catalyst [23,28,33].

The Sabatier reaction is a highly exothermic reaction with eight electron processes with considerable kinetic limitations [34,35]. Catalysts are necessary to overcome the activation barriers and achieve maximum CO_2 conversions at low enough temperatures, which is recommended based on the equilibrium conditions [34,35]. To prepare an effective and stable catalytic system, it is crucial to understand the reaction mechanism and its intermediate process [34]. For CO_2 methanation, the reaction step and the nature of the reaction intermediate are still being discussed in the literature [36–42].

The CO_2 methanation reaction, characterized by several elementary steps, displays varying reaction mechanisms that can be investigated through diverse in situ spectroscopic techniques and DFT theoretical calculations, contingent on the catalyst type. The process initiates with CO_2 adsorption onto the carrier, leading to interactions with hydroxyl groups, forming bicarbonate species. Concurrently, H_2 adsorbs onto metal sites, dissociating into H species. This step is followed by the hydrogenation of bicarbonate to yield formate species [43,44]. As depicted in Figure 2a, these formate species undergo hydrogenation into CH_4 via three distinct pathways.

The first pathway involves the further reduction of formate into adsorbed CO, aided by H in facilitating CO dissociation, thereby forming the (HCO_{ad}) intermediate. This inter-

mediate is then subjected to a series of consecutive hydrogenation reactions, culminating in CH_4 formation. Zhang et al. [43] identified the cleavage of the C=O bond in the (HCO_{ad}) intermediate on the Ni/CeO_2 (111) surface as the critical step in this process. Macroscopically, the primary reaction can be described as CO_2 undergoing RWGS to convert into CO, followed by hydrogenation into CH_4; hence, it is termed the RWGS + CO Hydro pathway.

The second pathway is analogous to the first in its initial steps and diverges as (CO_{ad}) dissociates directly into (C_{ad}) and O, with (C_{ad}) undergoing direct hydrogenation into CH_4, bypassing other intermediates. This is known as the CO pathway. Xinyu et al. [45] noted that the active sites on the Ni catalyst facilitate H_2 molecule dissociation into H atoms. They proposed that, on Ni/ZrO_2, CO_2 is activated by O_2 vacancies and transformed into adsorbed CO, which, along with H_2 activation on Ni, leads to CH_4 generation. Ren et al. [44] suggested that, on Ni (111) surfaces, the direct hydrogenation of CO_2 is the most efficient methanation route, with the $CO^* \rightarrow C^* + O^*$ transition as the rate-limiting step.

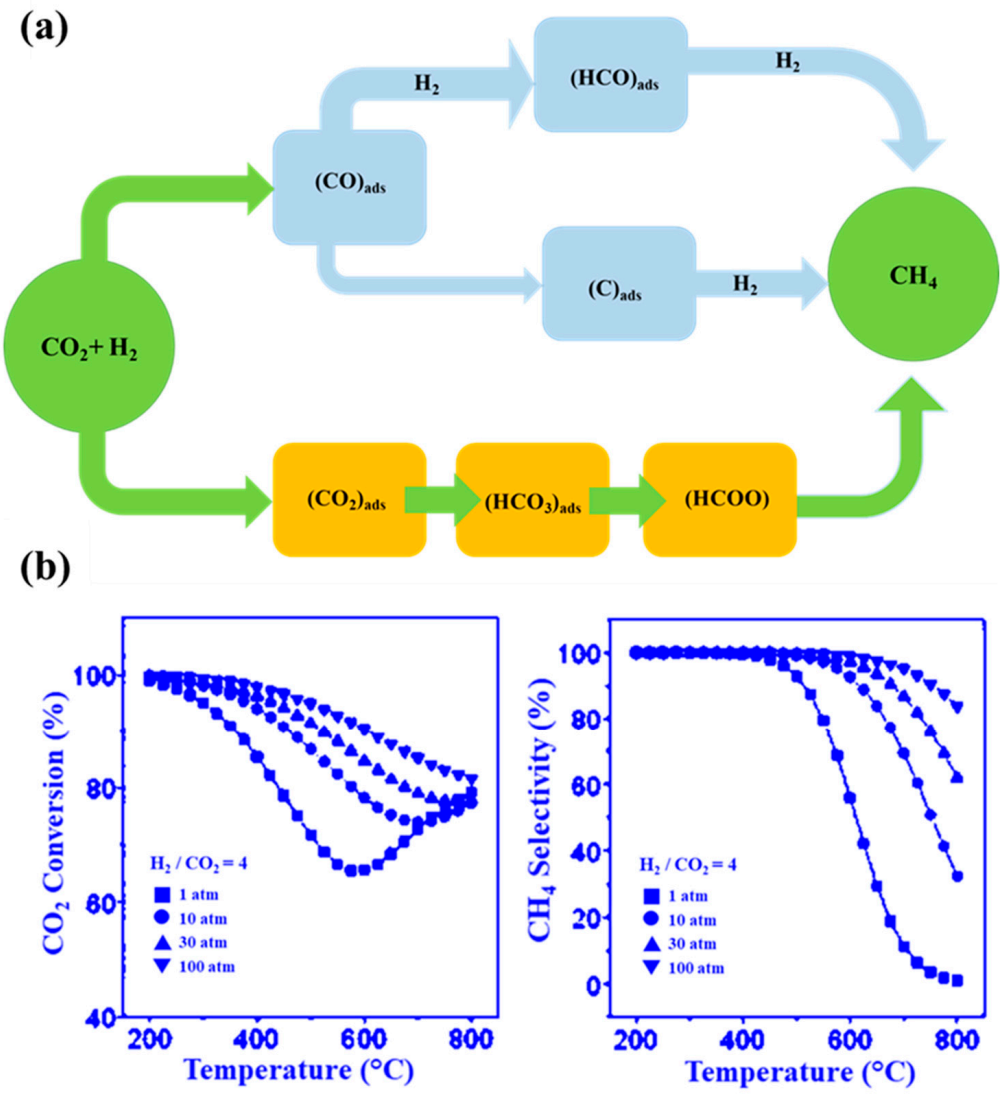

Figure 2. Reaction mechanism of CO_2 methanation: (**a**) reaction pathway; (**b**) thermodynamic equilibrium impact of pressure and temperature on CO_2 methanation [46].

The formate pathway, also referred to as the direct pathway, involves the direct interaction of CO_2 and H_2, resulting in the formation of a formate intermediate (HCOO) on the catalyst surface, as illustrated in Figure 2a. Notably, no CO intermediates are formed during this process [41,45]. A study conducted by Pan et al. [47] determined that the CO_2 methanation reaction pathways on $Ni/\gamma\text{-}Al_2O_3$ and $Ni/CeZrO_2$ catalysts both

followed the formate pathway but exhibited variations in terms of reactive basic sites. On the $Ni/CeZrO_2$ catalyst, CO_2 adsorption primarily occurred on medium basic sites, resulting in the formation of bidentate formate, whereas CO_2 adsorption on surface O_2 led to the creation of monodentate formate. The faster hydrogenation of monodentate formate suggested its dominance as the primary reaction route on the $Ni/CeZrO_2$ catalyst. In contrast, on $Ni/\gamma\text{-}Al_2O_3$, the principal reaction pathway involved the hydrogenation of bidentate formate, with the strong basic sites of $Ni/\gamma\text{-}Al_2O_3$ not actively participating in the CO_2 methanation reaction. It was proposed that medium basic sites play a crucial role in facilitating the formation of monodentate formate species, thereby enhancing the overall CO_2 methanation activity.

2.2. Thermodynamic Equilibrium Conversion and Selectivity

Several thermodynamic studies have examined the effects of reaction parameters on CO_2 methanation [34,36,48–51].

$$CO_2 + 4H_2 \rightarrow CH_4 + 2H_2O\ \Delta HR = -165\ \text{kJ mol}^{-1} \quad (1)$$

$$CO_2 + H_2 \rightarrow CO + H_2O\ \Delta HR = 41\ \text{kJ mol}^{-1} \quad (2)$$

$$CO + 3H_2 \rightarrow CH_4 + H_2O\ \Delta HR = -206\ \text{kJ mol}^{-1} \quad (3)$$

Understanding the CO_2 methanation reaction significantly relies on thermodynamic equilibrium. The CO_2 methanation reaction is a combination of the deceleration of exothermic (CO methanation) and endothermic (water gas shift) reactions, as shown in Equations (1)–(3) [52,53].

Lower temperatures are more favorable for the methanation reaction, leading to an increase in CO_2 conversion and an improvement in CH_4 selectivity [46,54]. The CO_2 methanation process exhibits the highest productivity at low temperatures, resulting in nearly 100% CO_2 conversion and CH_4 selectivity [55]. However, at higher temperature surpassing 500–600 °C, the dynamics shift toward a reversed water gas shift (RWGS) reaction, which results in a decrease in catalytic efficiency (depicted in Figure 2) due to carbon deposition [50,56].

In CO_2 methanation, the number of molecules decreases from five for reactants to three for products; therefore, the rise in pressure has a positive impact on CO_2 conversion, mainly when operating within temperature ranges of 200–500 °C [57]. High pressure is also favorable for CH_4 selectivity [46]. The effect of pressure can also be seen in Figure 2b, which presents thermodynamic equilibrium results. For the catalytic reaction, when the desorption of the product is the rate-limiting step, high pressure can suppress the reaction. Moreover, high pressure can increase equipment costs. CO_2 conversion and CH_4 selectivity are significantly influenced by the ratio of H_2 to CO_2. Higher ratios of H_2/CO_2 are associated with an increase in both the conversion of CO_2 and the selectivity toward CH_4 at 1 and 30 atm. Specifically, at a H_2/CO_2 ratio of two, the conversion of CO_2 ranges between 50% and 70% at both 1 atm and 30 atm. In these conditions, the selectivity for CH_4 reaches a maximum of 73% at 1 atm and 88% at 30 atm. Moreover, in this stoichiometric ratio, the yield of CH_4 can be observed to be around 40% at 1 atm, increasing marginally to 45% at 30 atm. The optimal conversion of CO_2 into CH_4 is achievable under conditions of low temperature and high pressure, provided that the H_2/CO_2 ratio is meticulously controlled. The enthalpy, entropy, and Gibbs free energy in standard conditions of both reactants and products are provided in Table 1.

Table 1. Enthalpy, entropy, and Gibbs free energy of reactants and products [57].

Substance	Enthalpy (ΔH)	Entropy (ΔS)	Gibbs Free Energy (Δ*G*)
	J/mol	J/mol.K	J/mol
CO_2	−393,509	214	−394,359
H_2	0	130.7	0
CH_4	−74,520	186.4	−50,460
H_2O	−241,818	188.3	−228,572

3. The Catalytic Performance of Noble Metal Catalysts in CO_2 Methanation

Numerous studies on using noble and non-noble metal catalysts to convert CO_2 into CH_4 have been proposed, and many of these have shown high activity and selectivity [58,59]. Ruthenium (Ru) and rhodium (Rh) show high activity with a comparatively small amount of metal loading at low temperatures [60]. Among the noble metals, Ru is the most active and stable catalyst for CO_2 methanation, next to Rh and Pd in order of activity [61]. Results from the representative published literature describing the patterns of activity, selectivity, stability, and corresponding reaction conditions are presented in Table 2.

3.1. Ruthenium-Based Catalysts

The catalytic performance of alumina-supported ruthenium (Ru/Al_2O_3) was investigated by Garbarino et al. [62], who observed that supported Ru catalysts are more active and stable than other metal-based catalysts. The supported Ru catalysts show excellent activity, especially at low temperatures, while the selection of the best catalyst preparation method and activation need to be carefully managed [63]. Ru/Al_2O_3 demonstrates high catalytic activity and good stability at 375 °C for 100 h, exhibiting 91% conversion and standing at 91% CH_4 selectivity. The superior activity and stability were attributed to the high dispersion of Ru nanoparticles (NPs) and interactions between Ru NPs and the Al_2O_3 support. The consistent and stable high activity observed after different shutdown and start-up sequences suggests that the catalyst retains its effectiveness even under intermittent operation [62].

Ru doped with ceria is one of the most promising methanation catalysts owing to the essential nature of the O_2 vacancies on the surface of CeO_2, which can activate CO_2. For Ru/Al_3O_2, adding ceria can improve the activity [64]. For Ce-doped Ru/Al_3O_2 catalysts, initial Ru NPs can be redispersed during oxidative pretreatment into atomically distributed RuOx species owing to interactions between Ru and ceria. The re-dispersion of Ru NPs on CeO_2 was also reported by Aitbekova et al. [65], and the re-dispersion could maintain the high activity of Ru NPs.

This reaction route was proposed to belong to the CO route, with CO_2 activated by O_2 vacancies and then converted into adsorbed CO; the CO and H_2 were activated by Ru to generate CH_4.

Besides CeO_2 and Al_2O_3, TiO_2 is also a promising support for loading Ru [66]. Researchers have demonstrated that TiO_2-supported Ru NP catalysts possess good stability, which is attributable to the unique interaction between metal Ru and support TiO_2. The CO_2 conversion can maintain stability for 34 h running, with 68% of CO_2 conversion and 98% selectivity to CH_4 at 290 °C and 1 atm. For Ru/TiO_2 catalysts, the catalytic performance relies on metal–support interactions, the loading amount of Ru, and the particle size of Ru NPs [67–71].

Table 2. Recent stable noble metal catalyst development for CO_2 methanation.

Catalyst	Preparation Methods	Metal Loading (%)	XCO_2 (mol%)	SCH_4 (mol%)	Period of Stable Running (h)	Reaction Conditions GHSV h^{-1}/WHSV ($mL.g^{-1}h^{-1}$)	T (°C)	Ref.
Ruthenium-based catalysts								
Ru/Al_2O_3	Commercial catalyst	3	91	91	100	55,000 * H_2:CO_2 = 5:1	375	[62]
Ru/CeO_2	Hydrothermal	5	86	100	30	30,000	300	[72]
Ru-Ni/Ce0.6Zr $0.4O_2$	Deposition precipitation	3/30	98	100	300	24,000	230	[73]
$Ru-CeO_2/Al_2O_3$	Impregnation	2	60	99	-	10,000	300	[74]
Ru/TiO_2	Impregnation	2.5	90	99	50	6000	350	[75]
Ru/TiO_2	Impregnation	5	68	98	34	7580	290	[67]
Ru/UiO-66	Impregnation	1	60	100	160	19,000	250 ** 5	[76]
Ru/TiO_2 (001)	Solvothermal hydrolysis	2.5	80	100	168	6000	325	[66]
$Ru/CeO_2/r$	Hydrothermal	3.7	75	99	24	72,000	350	[77]
Ru/CeO_2	Thermal deposition	-	83	90	14	-	225	[78]
Ru@MIL-101	Hydrothermal	-	90	99	48	-	225	[69]
Rhodium-based catalysts								
Rh/TiO_2	Impregnation	1	90	96	3	12,000	370 ** 2	[79]
$Rh/\gamma Al_2O_3$	Wet impregnation	1	25	100	-	-	125	[80]
RhY	Ion-exchange	6	59	99.8	2	60,000 * H_2:CO_2 = 3:1	150	[81]
Rh/CeO_2	Impregnation	3	~46	~100	-	-	350	[82]
Rh/Al_2O_3	Impregnation	1	25	100	-	-	250	[57]
Rh/PSAC	Impregnation	2	54	73	2	10,000	207	[83]
$PdRuNi/Al_2O_3$	Impregnation	2/8/90	53	40	5		400	[84]
RuRh-γ Al_2O_3	Impregnation	0.5/0.5	80	100	-	6000	250	[85]
Ni-Rh/Al_2O_3	Co-impregnation	10/0.5	65	92	4	57,000	300	[86]
Palladium-based catalysts								
Pd/UiO-66	Sol–gel	6	56	97.3	-	15,000	340	[87]
Pd/Al_2O_3	Impregnation	5	-	40	-	45,000	280	[88]
$PdO/LaCoO_3$	One-pot	3	62	99	2	18,000	300	[89]
$PdO/LaCoO_3$	Impregnation	3	32	87	2	18,000	300	[89]
$Pd-Mg/SiO_2$	Microemulsion	6.2	59	95	9	7320	450	[90]
Pd@FeO	Seeded growth	5.2	98	100	20 Rounds	-	180	[91]
$NiPd/Al_2O_3$	Co-impregnation	10–0.5	91	99	4	57,000	300	[86]

Notes: Reaction gas composition is H_2:CO_2 = 4:1, otherwise noted as *. Reaction Pressure is 1 bar, otherwise noted as **.

In one study using metal–organic frameworks (MOFs) with Ru metal as a precursor and silica nanofibrous veils (MIL-101) as the support, the resulting Ru@MIL-101 catalyst showed good catalytic performance with a CO_2 conversion of 90% and a selectivity to CH_4 of 99%, and it maintained stability for 48 h under conditions of 1 bar and 225 °C [69]. The high activity is attributable to the high dispersion of Ru NPs and the stability owes to the interaction between Ru and the silica support [69].

The best catalytic performance is shown on Ru-Ni/$Ce_{0.6}Zr_{0.4}O_2$ with 3 wt.% Ru loading: CO_2 conversion reaches 98%, the CH_4 selectivity is 100%, and the stability period is 300 h under reaction conditions of a GHSV/WHSV of 24,000 ($mLg^{-1}h^{-1}$), 230 °C, and 1 bar [73].

3.2. Rhodium-Based Catalysts

For Rh-based catalysts, the best performance is shown on Rh/TiO_2 with 1 wt.% of Rh loading, which exhibits 90% CO_2 conversion and 96% selectivity to CH_4 with only 3 h of stability running under reaction conditions of a GHSV/WHSV of 12,000 h^{-1} ($mL.g^{-1}h^{-1}$), 370 °C, and 2 bar [79]. Considering the high reaction temperature and pressure, the activity of Rh is inferior to that of Ru; furthermore, investigations on the stability of Rh-based catalysts for CO_2 methanation have not been extensively covered in the literature.

Moreover, the activity of Rh-based catalysts has been improved by adding other active metals, such as Ru-Rh/Al_2O_3, showing better activity than mono Rh [85], and Ni-Rh/Al_2O_3 also exhibits better activity than Rh/Al_2O_3 [86].

Catalytic performance may be affected by the O_2 presence; O_2 in a low percentage boosts the catalyst's performance, whereas a higher concentration leads to a negative ef-

fect [56,92]. Martin et al. [82] investigated the effects of support on Rh for CO_2 methanation reactions; Rh NPs were loaded on SiO_2, Al_2O_3, and CeO_2, and they found that CeO_2 and Al_2O_3 exhibited better activity than SiO_2. Furthermore, researchers have discovered that the catalytic performance of Rh/Al_2O_3 catalysts is dependent on Rh particle sizes ranging from 3.6 nm to 15.4 nm [49,59].

TiO_2 is one of the best options for supporting Rh catalysts. The effects of Rh/TiO_2 on catalytic performance at low temperatures were investigated by Alejandro et al. [93], who found that large Rh particle sizes have more active sites and weak CO intermediates, which also affects the order of CO_2 methanation reaction and activation energies. Notably, a slight variation in the activation energy of CO dissociation with Rh particle size was observed. Higher response orders in H_2 were also seen for smaller particles, indicative of reduced H_2 coverage. CH_4 selectivity gradually increased with a change in particle size (from 2 nm to 7 nm), while, beyond this particle size, there was no discernible difference [93].

It has been observed that Rh/TiO_2 catalysts have higher CH_4 selectivity as compared with Rh/Al_2O_3 and Rh/SiO_2. The literature suggests that the breakdown of the C-O bond could be aided by electron interactions between metal and supports or interactions between CO absorbed by a catalyst and Ti 3^+ ions positioned at the border metal support [79,93].

Jiang et al. [79] further investigated the influence of different oxide supports (TiO_2, Al_2O_3, and ZnO) on the catalytic activity of Rh catalysts in CO_2 methanation and indicated that the selection of a suitable support significantly affects the performance of Rh catalysts. Rh/TiO_2 exhibited the highest catalytic activity over a 6 h duration stability, followed by Rh/Al_2O_3 and Rh/ZnO. Variations in the electronic structure of the metallic Rh and its interaction with oxide supports can be linked to this discrepancy in activity. The TiO_2 support of Rh-based catalysts enhances electron transport to Rh NPs, resulting in more marked CO dissociation and catalytic activity. In contrast, electron transport happens to the support, or it remains localized in Rh/ZnO and Rh/Al_2O_3 catalysts, resulting in a decrease in catalytic efficiency. These findings highlight the significance of electronic structure modulation and support effects in designing efficient CO_2 conversion catalysts.

Research on Rh/TiO_2 by Martnez et al. [68] showed that changes in activity depend on interactions between Rh NPs and the support. The average particle size after H_2 reduction at a high temperature is substantially smaller than the size of calcined Ru in the presence of synthetic air and then further heated at 300 °C, which was confirmed with TEM and XRD [68]. The interaction can make Rh re-disperse, which leads to the high dispersion state of Rh NPs, resulting in higher CO_2 conversion.

Scientists have turned to innovative mesoporous Rh NPs synthesized using a wet chemical reduction technique [59]. The mesoporous Rh catalyst is more active than the nonporous Rh catalyst in the CO_2 methanation reaction. The high density of atomic steps on the mesoporous Rh catalyst is responsible for its higher catalytic activity with 99% CO_2 conversion and 96% CH_4 selectivity [94].

3.3. Palladium-Based Catalysts

For Pd-based catalysts, the best catalytic performance was shown on Pd@FeO with a Pd loading amount of 5.2 wt.%, showing 98% CO_2 conversion and 100% selectivity to CH_4 at a low temperature of 180 °C, and the catalytic performance was maintained for 20 rounds of cyclic running [91]. The high activity was attributed to the face-centered tetragonal structure of the Pd-Fe intermetallic nanocrystal, and it was proposed that Pd-Fe intermetallic nanocrystals aided in maintaining metallic Fe species during CO_2 methanation via a reversible oxidation-reduction mechanism; thus, adding metallic Fe facilitated the direct conversion of CO_2. This study was efficient on a laboratory scale, but for practical applications, the loading amount of Pd is too high, and the stability needs to be investigated.

The bimetallic catalysts of Ni-Pd supported on Al_2O_3 show better activity with 0.5 wt.% and 10 wt.% loadings of Pd and Ni, respectively. In one study, a CO_2 conversion of 91% and 99% CH_4 selectivity was achieved under reaction conditions of a GHSV/WHSV of 57,000 ($mL.g^{-1}h^{-1}$), 300 °C, and 1 atm, and it remained stable for 4 h [86].

Jiang et al. [87] investigated Pd NPs supported on MOFs and found a synergistic interaction between the metal and the support, which improved the catalyst's performance and exhibited higher CO_2 conversion and CH_4 selectivity at 340 °C with 6 wt.% Pd loading compared with individual Pd NPs or UiO-66. Apart from the high loading of Pd, the metal–organic compound UiO-66 is unstable for long periods in CO_2 methanation reactions because CO_2 reacts with organics [95,96].

It was reported that, on Pd/Al_2O_3 catalysts, CO_2 methanation is a structure-sensitive reaction; as noted by Wang et al. [93], by stabilizing CO species on the terrace sites of Pd NPs, CH_4 generation can be effectively enhanced. They proposed that the arrangement of Pd atoms on the surface affects the adsorption strength of reactants and CO intermediates, resulting in significantly boosted CH_4 selectivity.

3.4. Summary of Performance of Noble Metal Catalysts

Studies on noble metal catalysts for CO_2 methanation have mainly concentrated on Ru-, Rh-, and Pd-based catalysts, among them Ru based catalysts exhibited the best catalytic performance. For all catalysts, selectivity to CH_4 can be very good, especially at low reaction temperatures, so the challenge is to enhance the activity at low temperatures. When the loading amount of noble metal is as high as 3–6 wt.%, much higher CO_2 conversion can be achieved, although the high price means it has promise in practical applications. Ru-based catalysts have shown comparatively good stability in maintaining stability for 300 h running, but stability investigations of Rh- and Pd-based catalysts are needed.

Research on noble metal catalysts for CO_2 methanation has predominantly focused on Ru-, Rh-, and Pd-based catalysts; among them, Ru-based catalysts demonstrate superior catalytic performance. These catalysts generally exhibit high CH_4 selectivity, particularly at low reaction temperatures. However, enhancing activity at low temperatures remains a challenge. Notably, when the noble metal loading reaches 3–6 wt.%, a significant increase in CO_2 conversion can be observed. Nonetheless, the economic feasibility of such high loadings is questionable given the consequent increase in costs, limiting practical applications. While Ru-based catalysts have shown relatively better stability, maintaining catalytic performance for 300 h, the stability of Rh- and Pd-based catalysts needs to be further investigated.

The catalytic performance of noble metal catalysts has been found to be dependent on metal dispersion, metal–support interactions, and morphology, and bimetallic or intermetallic nanocrystals seem to be a promising route for improving catalytic performance.

4. The Catalytic Performance of Non-Noble Metal Catalysts in CO_2 Methanation

Extensive research has been conducted to identify alternative catalyst materials given the scarcity and high costs of noble metals. Non-noble metals, mainly Ni, Co, and Fe. have acquired considerable attention for their potential in CO_2 methanation [97–99]. In the following sections, the application of non-noble metal catalysts, nickel (Ni), cobalt (Co), and iron (Fe), in the Sabatier reaction are investigated. Research is being conducted in order to optimize their catalytic performance, optimize their activity, and investigate the factors affecting their stability.

4.1. Nickel-Based Catalysts

Ni-based catalysts have gained significant attention in CO_2 methanation. The research emphasis has been on enhancing its activity in low reaction temperatures and improving the sintering resistance of Ni NPs because of the inert nature of CO_2 and the strong exothermic activity of the methanation reaction. In designing a promising catalyst for industrial applications, the critical factors of catalytic performance are the properties of Ni NPs, including dispersion and its chemical state, metal–support interactions, and additive materials. Supports such as Al_2O_3 [62,100], SiO_2 [64,101], TiO_2 [102,103], ZrO_2 [104,105], CeO_2 [106,107], and the solid solution Ce-Zr-O [108] are predominantly utilized for loading Ni NPs. The additives mostly employed are alkaline earth metals, such as La, Y, and Ce;

the basic element Mg; the transition element Mn; and so on. Catalyst synthesis methods are diverse, with the principal objectives being to increase Ni NP dispersion and/or adjust interactions between Ni NPs and the support or additives. Examples of the catalytic performance of Ni-based catalysts are presented in Table 3.

Al_2O_3 is the most frequently applied catalyst support for CO_2 methanation [109,110]. Al_2O_3 is extensively used owing to its high surface area, adjustable porous structure, and complex chemistry properties [99,111,112]. Therefore, Al_2O_3 is not suitable for loading Ni NPs for CO_2 methanation, but reports on Ni/Al_2O_3 for CO_2 methanation are significant [113,114]. An issue with using Al_2O_3 as a support for the methanation reaction is that it tends to sinter when exposed to water (a byproduct of the process) at high temperatures [99].

The activity of Ni/Al_2O_3 is not good enough; with a loading of 12.5 wt.% Ni on Al_2O_3, CO_2 conversion could reach 71% at a high temperature of 500 °C [115], and the reason for the poor activity can likely be attributed to the poor CO_2 activation ability of Al_2O_3. When adding an additive to activate CO_2, such as ceria, the activity could be improved effectively over Ni/CeO_2-Al_2O_3; 71% CO_2 conversion and 99% selectivity to CH_4 could be achieved at a low temperature of 350 °C, at reaction conditions of a GHSV/WHSV of 15,000 ($mL.g^{-1}h^{-1}$) and 1 atm [116].

Silica (SiO_2) is another popular choice since it has a large surface area and may adjust its pore diameter to suit a given application [117–119]. Ni and SiO_2 form metal–support interactions, which are antagonistic to the growth of Ni carbide, which leads to the improved catalyst's resistance to coke production and Ni sintering. [120,121]. In the literature, CO_2 methanation with a SiO_2-supported catalyst has shown a CO_2 conversion efficiency of only about 60% to 90% [90,122–125], which may be due to the inertness of SiO_2; therefore, the additive addition or surface modification of the support needs to be further investigated [126,127].

Moghaddam et al. [128] demonstrated that Ni NPs loaded on a composite support made of Al_2O_3-SiO_2 showed much better catalytic performance at 350 °C. A CO_2 conversion of 82% and a CH_4 selectivity of 98% were achieved, and constant performance was maintained for over 30 h. The good activity and stability of this catalyst can be attributed to the formation of highly dispersed Ni NPs and interactions between Ni NPs and the support, respectively [128].

Similar to studies that used alumina-supported Ni catalysts, Li et al. used Mg as a promoter for Ni/SiO_2; the resultant catalyst showed obviously improved activity with 82% CO_2 conversion and 99% selectivity to CH_4 under reaction conditions of a GHSV/WHSV of 60,000 ($mL.g^{-1}h^{-1}$), 250 °C, and 1 atm [129]. SiO_2 with a high surface area and a mesoporosity of MCM-41 is sufficient support for CO_2 methanation. A high surface area favors the high dispersion of Ni NPs, and mesoporosity is beneficial for reactant transfer [110,130].

For example, Ni/MCM-41 showed 56% CO_2 conversion and 98% selectivity to CH_4 under reaction conditions of a GHSV/WHSV of 50,000 ($mL.g^{-1}h^{-1}$), 250 °C, and 1 atm [131]. At the same time, it has been observed that improved resistance to coke formation can be achieved with a high surface area, and it is also known that carbon deposition formation can be suppressed on highly dispersed Ni NPs supported on SiO_2[132].

Table 3. Recent developments in non-noble catalysts.

Catalyst	Preparation Methods	Metal Loading	XCO_2	SCH_4	Period of Stability	Reaction Conditions		Ref.
		(%)	(mol%)	(mol%)	(h)	GHSVh^{-1}/WHSV mL.$g^{-1}h^{-1}$	T (°C)	
Nickel-based catalysts								
Ni/Al_2O_3	Impregnation	20	80	100	10	9000	350	[133]
Ni/Al_2O_3	Improved one-pot EISA	10	60	95	60	10,000	400	[134]
Ni/Al_2O_3	Impregnation	30	71	95	24	30,000 * H_2:CO_2:Ar = 61:15: 21	350 ** 2	[135]
Ni/Al_2O_3-SiO_2	Sol–gel	30/0.5	82	98	30	12,000 H_2:CO_2 = 3.5:1	350	[128]
Ni-Co/Al_2O_3	Improved one-pot EISA	10/3	70	96	60	10,000	400	[134]
$NiFe/Al_2O_3$	One-pot-induction EISA		84.1	100	150		420	[136]
Ni-Pt/γ-Al_2O_3	Co-impregnation	10–0.5	83	97	60	5700	250	[86]
Ni-Pd/γ-Al_2O_3	Co-impregnation	10–0.5	91	97	30	5700	250	[86]
Ni/Al_2O_3-ZrO_2	Sol–gel	20	76	100	100	20,000	300	[137]
Mn-Ni/Al_2O_3	Impregnation	1.71	66	100	-		300	[138]
Ni-Pr/Al_2O_3	Impregnation	12–5	98	100	48	6000	300	[139]
Ni-Ce/Al_2O_3	Impregnation	15–15	70	98	80	30,000	350	[116]
NiO/SiO_2	Sol–gel	60	86	95	48	10,000	350	[140]
Ni-La_2O_3/SiO_2	Citric complex	7.7	89	90	400	15,000	500	[141]
$NiLaMoO_3/SiO_2$	Citric complex	6	87	100	320	15,000	350	[121]
Ni/MSN	Sol–gel	5	64	100	200	50,000	300	[130]
Ni/MOF-5	Impregnation	10	75	100	100	2000	320	[142]
Ni/MSN	Impregnation	5	64	100	100	50,000	300	[131]
Ni@HZSM-5	Hydrothermal	20	64	99	40	36,000	400	[143]
Ni/OMA	Impregnation	15	87	98	150	91,000 * H_2:CO_2 = 5:1	400	[144]
Ni/CNT	Co-impregnation	12	61	97	100	30,000	350	[145]
Ni/3D-SBA-15	Impregnation	15	86	99	100	60,000	400	[146]
Ni/C.Z.	Pseudo sol–gel	5	80	99	90	43,000	350	[37]
HTNiCu	Co-precipitation	15	86	98	72	12,000 * H_2:CO_2:Ar = 6:1.5:2.5	350	[147]
Ni-Ce-Y/SBA-15	CTAB-assisted impregnation	15–10	61	97	26		350	[148]
NiMg/USY	Ion exchange	13–9	65	92	10	12,000 * H_2:CO_2:Ar = 36:9:10	400	[149]
Ni-Mn/Bn-U	Solution combustion synthesis		85	100	150	36,000	270	[150]
Ni-La	Urea hydrolysis	15	85	94	150	45,000	350	[151]
Ni-La	Impregnation	13.6–14	90	100	8	55,000 H_2:CO_2 = 5:1	350	[152]
Ni/TiO_2	Deposition precipitation	15	80	96	81	18,000 * H_2:CO_2:Ar = 12:3:5	340	[153]
Ni/Y_2O_3	Impregnation	10	80	100	50	20,000	300	[110]
Ni/ZrO_2	Impregnation	15	60	100	50	48,000	300	[154]
Ni/ZrO_2	Plasma decomposition	5	79	77	70	60,000	350	[45]
Ni/ZrO_2	Impregnation	10	74	71	10	60,000	400	[45]
Ni/CeO_2	Sol–gel	20	81	96	106	40,000	250	[155]
Ni/CeO_2	Hard template	10	91	100	11	22,000	340	[107]
Ni/CeO_2-	Impregnation	10	93	100	14	10,000	350	[64]
Ni-$Ce_{0.2}Zr_{0.8}O_2$	Citric Complex	15	71	100	200	15,000	250	[108]
Ni-$Ce_{0.72}Zr_{0.28}O_2$	Sol–gel	15/0.6	90	98	150	21,000	350	[156]
Ni/CeO_2-ZrO_2	Ammonia evaporation	10	55	99.8	70	20,000	275	[157]
Ni/CeO_2-ZrO_2	Colloidal dispersion	2	58	98	60	60,000 * H_2:CO_2:He = 12:3:5	350	[158]
Ni/CeO_2-ZrO_2	Pseudo-sol–gel	5	68	98		43,000	350	[37]
$Ni/Ce_{0.6}O_2Zr_{0.4}O_2$	Co-precipitation	15/0.6	71	86	83	12,500	300	[159]
$Ni/Ce_{0.75}Zr_{0.25}$		25	85	—	30.		300	[160]
Ni-$La_2O_3CeO_2/ZrO_2$	Citric Complex	-	80	100	160	15,000	350	[161]
Ni/ZrO_2-Al_2O_3	Co-impregnation	12	70	100	100	8100	360	[113]
Ni/CeO_2-Al_2O_3	Co-impregnation	15	71	99	120	15,000	350	[116]
Ni/CeO_2-Al_2O_3	Co impregnation	13	85	99	120	15,000	350	[162]
Cobalt- and iron-based catalysts								
Co-Pt/Al_2O_3	Double flame spray Pyrolysis	0.03	70	98	210	36,000	400	[163]
$NiCo/Al_2O_3$	Impregnation	20	90	100	200	13,000	325	[164]
Ni-Co/Al_2O_3	Solid-phase synthesis	15–12.5	76	96	10	9000	400	[165]
Ni-Co/Al_2O_3	Impregnation	10–10	61	95	200	13,000	350	[164]
$NiCoMgZnMn/Al_2O_4$	Citric complex	6.8/9.8	64	100	320	15,000	350	[166]
Co_3O_4 nanorod	Co-precipitation		70	99	50	18,000 H_2:CO_2 = 4:6	330 ** 10	[167]
Co/KIT-6	Excess impregnation	20	48.9	100	-	22,000	280	[33]
CoNR/TiO_2	Modular synthesis	-	57	100	72	18,000	250 ** 10	[168]
$(Co_{0.95}\ Ru_{0.05})O_4$	Modified wet chemistry protocol	-	34.2	97.4	50	21,240	420	[167]
PrCoPal	Impregnation		68	95	200	150,000	350	[169]
Co/ZrO_2	Wetness impregnation	10	92	99	300	3600	400 ** 30	[170]
Co/ZrO_2	Citric complex	2	85	99	300	7200	400 ** 30	[171]
Co-$Zr_{0.1}$B-O	Liquid-phase synthesis	-	78	98	12	20,000	180	[172]
$NiFe/Al_2O_3$	Impregnation	13–9	84.1	100	150	50,000	420	[136]
$NiFe/Al_2O_3$	One-pot sol–gel	30–5	71	99	10	9000	350	[173]
NiFe	Single-step co-precipitation	3–0.5	78		30	20,000	200	[174]
Ni_8Fe_2	Co-precipitation	30	80	95	200	10,000	150	[175]

Notes: Reaction gas composition is H_2:CO_2 = 4:1, otherwise noted as *. Reaction Pressure is 1 bar, otherwise noted as **.

Zhen et al. [142] investigated the effect of O_2 vacancies on the reaction mechanisms of Ni NPs supported on SiO_2 with a high surface area and found that O_2 vacancies could be formed on the surface of the SiO_2 support, which could activate CO_2 to then improve the catalytic performance.

The distinctive catalytic performance of SiO_2 with a high surface area loaded with Ni NPs has naturally inspired researchers to investigate zeolite as a support for CO_2 methanation, as it is known that a key characteristic of silica zeolite is a high surface area. Chen et al. [143] used a conventional Ni/SiO_2 as a precursor-prepared core–shell catalyst for Ni@HZSM-5 via the hydrothermal method. Compared with traditionally prepared Ni/SiO_2 and Ni/HZSM-5 catalysts, Ni@HZSM-5 exhibited superior performance, preserving its Ni content and the structure of the active Ni after a 40 h CO_2 methanation reaction. A key feature of this catalyst is the interaction between the Ni active phase and zeolite, with the former donating more electrons to the latter, thus preventing sintering and enhancing the activity of Ni. At 400 °C, the Ni@HZSM-5 catalyst demonstrated a CO_2 conversion of 64% and near 100% CH_4 selectivity under reaction conditions of a GHSV/WHSV of 36,000 ($mL.g^{-1}h^{-1}$), 400 °C, and 1 atm [131].

Dong and Liu [146] developed a three-dimensional-ordered (3D) macroporous SBA-15-loaded Ni catalyst. As is known, SBA-15 is a silica zeolite, and making SBA-15 into a 3D macroporous can lead to a high surface area accompanied by macropores for transferring. The resultant catalyst showed high catalytic performance for CO_2 methanation, achieving a CO_2 conversion of 80% and selectivity to CH_4 of 98% under reaction conditions of GHSV/WHSV of 36,000 ($mL.g^{-1}h^{-1}$), 400 °C, and 1 atm, and it maintained its performance over an extended period of 120 h.

Generally, SiO_2 is an inert support; therefore, adding basic elements could help to activate CO_2. Gong et al. [141] added La_2O_3 to Ni/SiO_2 for CO_2 methanation and achieved a CO_2 conversion of 89% and a selectivity to CH_4 of 90% under reaction conditions of a GHSV/WHSV of 15,000 ($mL.g^{-1}h^{-1}$), 500 °C, and 1 atm, and it remained stable for 400 h. The addition of lanthanum improved the dispersion and reducibility of the Ni ions, which significantly improved its activity. The SiO_2 support provided good stability and improved resistance to carbon deposition. The addition of SiO_2 as a support, along with lanthanum, considerably increased catalytic activity and stability.

Zirconia is a promising support for industrial applications because of the basic properties of ZrO_2, which can activate CO_2. Moreover, ZrO_2 possesses high thermal stability and can be prepared with high porosity and a large surface area [110]. Ni-supported ZrO_2 aids in forming active sites and increases O_2 vacancies on ZrO_2, which are also crucial for CO_2 methanation [171,176]. According to the literature, the dispersion of Ni NPs and particle reductions are supported by the high specific surface area of ZrO_2. CO_2 methanation reactions will vary depending on the polymorphic structure of the support (monoclinic, tetragonal, or cubic). Tetragonal ZrO_2 is the functional structure as catalyst support [177]. Preparing tetragonal ZrO_2 is challenging given its structure sensitivity. O_2 vacancies in m-ZrO_2 are more abundant, making it an effective catalyst for the CO_2 methanation reaction than t-ZrO_2 [105].

Tan et al. [178] prepared highly dispersed Ni NPs supported by MgO-doped ZrO_2; the resultant catalyst exhibited outstanding activity in CO_2 methanation, a CO_2 conversion of 90%, and a selectivity to CH_4 of 100% under reaction conditions of a GHSV/WHSV of 15,000 ($mL.g^{-1}h^{-1}$), 250 °C, and 1 atm, and it remained stable for 110 h. Ren et al. showed that 30% Ni supported on ZrO_2 could convert around 90% of CO_2 at 250 °C with 95% selectivity toward CH_4 [179]. High activity and selectivity were observed in Ni supported on t-ZrO_2 for methanation reactions between 200 and 300 °C. Catalytic activity rises with increasing t-ZrO_2 content, and the highest CH_4 selectivity can be achieved at 300 °C using tetragonal ZrO_2 prepared with Ni-Zr alloy [92].

CeO_2 is another extensively investigated support or additive for CO_2 methanation, owing to the fact that O_2 vacancies can be formed on the surface of ceria and the fact that the interaction between Ni NPs and ceria can promote a reduction in Ni ions and the dispersion

of Ni NPs [64,80,107,155,156,180–186]. Ye et al. [155] conducted a comprehensive study on using a nanostructured Ce-supported Ni-based catalyst prepared using the sol–gel method for CO_2 methanation. The findings highlight the extraordinary performance of this catalyst at a relatively modest temperature of 250 °C, yielding a CO_2 conversion ratio of 81% and a CH_4 selectivity of 96%, which could be maintained for 106 h. The good stability was attributed to the interaction between Ni NPs and CeO_2.

Both TiO_2 [64] and MOF [142] materials as support for CO_2 methanation have also gained some attention. The activity of Ni/TiO_2 is generally inferior compared with Ni/ZrO_2. For MOFs and carbon materials, the stability is not good enough because CO_2 can react with these materials.

Tada et al. conducted experiments comparing Ni NPs loaded on different supports made of CeO_2, Al_2O_3, TiO_2, and MgO [64]. They found that Ni/CeO_2 exhibited maximum CO_2 conversion across the usual temperature range, approaching an equilibrium value above 300 °C. Selectivity for CH_4 was nearly maximized at 100%. The catalyst performance of Ni/CeO_2 was attributed to the adsorption of CO_2 on O_2 vacancies in ceria and the high dispersion of Ni NPs [187]. The trend of the activity for different supports is as follows under the same reaction conditions: $Y_2O_3 > Sm_2O_3 > ZrO_2 > CeO_2 > Al_2O_3 > La_2O_3$.

A solid solution of Ce-Zr-O, which can be obtained via solid reactions between CeO_2 and ZrO_2, is the best support for loading Ni NPs for CO_2 methanation [186–190]. Sun et al. [108] analyzed how $Ni/CeZrO_2$ is the most predominant catalyst for CO_2 methanation reactions. Ni NPs on Ce-Zr-O solid solutions convert CO_2 more efficiently than pure CeO_2 and ZrO_2, of which $Ni/CeO_{0.2}Zr_{0.8}O_2$ catalyst has the highest CO_2 conversion rate (14% at 200 °C) and CH_4 selectivity (100% at 250 °C). Furthermore, Ni NPs supported on Ce-Zr-O solid solutions showed better stability than Ni NPs on CeO_2 or ZrO_2 [108].

Li et al. [161] investigated CO_2 methanation employing cerium-modified Ni supported on lanthanum oxide and zirconia ($Ni\text{-}La_2O_3\text{-}CeO_2/ZrO_2$). Their study focused on improving catalytic activity and stability. The study found that the addition of cerium to $Ni/La_2O_3\text{-}ZrO_2$ can enhance the dispersion and reducibility of Ni NPs, leading to higher catalytic activity and stability for 160 h.

Considering the comparatively high price, rare earth metal oxides such as Y_2O_3, Sm_2O_3, CeO_2, and La_2O_3 are not suitable for use as supports. In view of their characteristics, some of the reported supports, such as La_2O_3 and MgO, are unstable; preparing high surface area CeO_2 is a challenge; etc. However, the oxides of these are likely good additives. Thus, promising catalysts for CO_2 methanation for industrial applications are Ni NPs loaded on Al_2O_3, SiO_2, or ZrO_2, accompanied by some additives.

4.2. Cobalt-Based and Iron-Based Catalysts

Co-based catalysts are the most well-studied active component of Fischer–Tropsch synthesis (FTS), which generates hydrocarbons from syngas (a gas mixture of CO and H_2), as CO_2 can be converted into CO via reverse water gas shift reactions; therefore, studying Co-based catalysts for CO methanation is expected [191,192]. However, according to several studies, only a select few Co-based catalysts can concurrently achieve high CO_2 conversion, selectivity to CH_4, and stability, as shown in Table 3 [167,168,193–195].

Tu et al. [172] reported in their investigation that adding a Zr promoter allowed an amorphous $Co\text{-}Zr_{0.1}\text{-}B\text{-}O$ catalyst to initiate CO_2 methanation at temperatures as low as 140 °C. Maximum catalytic activity was achieved at 180 °C with 78% CO_2 conversion and 98% CH_4 selectivity, but the stability exhibited only lasted for 12 h.

In another study, Co/ZrO_2 showed good catalytic performance with 92% CO_2 conversion and 99% selectivity to CH_4, and this performance was maintained for 300 h under reaction conditions of a GHSV/WHSV of 36,000 ($mL.g^{-1}h^{-1}$), 400 °C, and 30 atm [170]. Considering the low space velocity, high pressure, and comparatively high temperature in these reaction conditions, the activity is very good but not excellent compared with Ni-based catalysts, although the stability seems very good.

Another study on Co-ZrO_2 for CO_2 methanation indicated that decreasing the particle size of Co, increasing Co dispersion, and strengthening the interaction between Co and ZrO_2. can improve activity, attributable to interactions between Co and ZrO_2, possibly generating more catalytically reduced active sites in Co and more O_2 vacancies, resulting in higher CO_2 adsorption (owing to O_2 vacancies) and high catalytic hydrogenation (owing to Co) [167].

Recent research on CO_2 methanation has revealed that adding a small number of catalytic promoters (Cu, Fe, La, Pr) significantly increases the catalyst's performance and stability, as determined in experimental and DFT analyses. Using a straightforward impregnation technique, a series of lanthanide-modified Co-palygorskite composites (LnCo-Pal, Ln–La/Ce/Pr/Sm) for CO_2 methanation under atmospheric pressure were developed. The CO_2 conversion of the PrCoPal catalyst was 68%, the selectivity to CH_4 was 95%, and it exhibited 200 h of stability under reaction conditions of a GHSV/WHSV of 15,000 ($mL.g^{-1}h^{-1}$), 350 °C, and 1 atm [169].

The most promising Co-containing catalysts for CO_2 methanation are bimetallic Ni-Co-based catalysts. Alrafei et al. [164] investigated a bimetallic 10%Ni-10%Co/Al_2O_3 catalyst prepared according to incipient wetness impregnation, and the catalyst exhibited very good performance in converting CO_2 into CH_4, with a 61% conversion rate and a 95% selectivity achieved at a relatively low temperature of 350 °C, and it maintained stability for 200 h with GHSV/WHSV of 13,000 ($mL.g^{-1}h^{-1}$) and 1 atm. The good stability was attributed to the interaction between the Ni-Co alloy NPs and the Al_2O_3 support (which inhibited the clustering of active Ni-Co alloy NPs) and to the Ni-Co alloy's resistance to carbon deposition. Incorporating Co into the Ni catalyst enhanced the reducibility of the Ni species and the distribution of Ni particles across the support, which increased activity.

High-entropy oxides (HEOs), defined as single-phase oxide systems containing a minimum of five distinct cations, exhibit unique properties advantageous to catalytic CO_2 methanation. The incorporation of diverse cations within the same lattice phase leads to a synergistic interaction, significantly enhancing their catalytic activity [165,166]. The cocktail effect leverages the diverse chemical environments created by interactions between cations. Additionally, the high dispersion of these elements within the lattice, thermal stability, an abundance of surface defects, and the synergistic effects of multielement interactions position HEOs as effective catalyst carriers. Significantly, HEOs are proving to be highly effective as precursors for catalysts, primarily because of their exceptional elemental dispersion. Chen et al. [165] incorporated platinum into a CoNiMgCuZnOx-based HEO via co-deposition, resulting in a catalyst with notable activity in CO oxidation and remarkable thermal stability, a testament to the entropic stability inherent to HEOs. The recent research conducted by Liu et al. [166] investigated the application of a remarkably stable bimetallic catalyst comprising Ni-Co supported on alumina-coated spinel oxide, derived from HEO (CoNiMgZnMg/Al_2O_4), for CO_2 methanation. The study revealed the exceptional stability and elevated catalytic efficiency of this Ni-Co/alumina–spinel catalyst for CO_2 methanation.

A viewpoint proposed in this paper needs to be noted: the active metals Co and/or Ni can be oxidized into metal ions, resulting in the deactivation of the catalyst. Different from CO methanation, in the process of CO_2 methanation, CO_2 can oxidize metallic NPs, and the resulting metal ions may react with the support to form a composite oxide, such as Co ions reacting with alumina to form $CoAl_2O_4$ spinel.

In the context of Fe-based catalysts, research indicates that pure Fe exhibits limited effectiveness in converting CO_2 into CH_4. However, when Fe is combined with Ni to form a bimetallic or alloy structure, the resulting combinations often perform better than pure Ni catalysts [36,196].

In a study by Moghaddam et al. [173], Ni/Al_2O_3 catalysts were prepared using the one-pot sol–gel method, with small amounts of additional elements such as Fe, Co, Cu, Zr, and La added. The catalyst containing Fe demonstrated exceptional performance, achieving 71% CO_2 conversion and nearly 99% selectivity for CH_4 at 350 °C, a GHSV/WHSV of

9000 (mL.g^{-1}h^{-1}), and 1 atm. This improvement can be attributed to the presence of a Ni-Fe alloy, which enhanced the adsorption of H_2 and the dissociation of CO_2. Interestingly, increasing the Fe content from 5 to 7 wt.% resulted in enhanced activity at lower temperatures and maintained stability over a 10 h period.

Yin et al. [174] investigated the effects of adding Fe to Ni-based catalysts for low-temperature CO_2 methanation. Different amounts of Fe were introduced, and it was found that a small amount (Ni3Fe0.5) significantly improved the catalyst's performance, achieving a CO_2 conversion of 78% at 200 °C, a GHSV/WHSV of 20,000 (mL.g^{-1}h^{-1}), and 1 atm. However, an excessive amount of Fe (1.5 wt.%) led to the formation of a detrimental $NiFe_2O_4$ spinel phase. The optimal amount of Fe addition was determined to be 0.5 wt.%, effectively enhancing the reducibility and basicity of the catalytic system. This facilitated CO_2 adsorption and activation, resulting in improved CO_2 methanation activity, which exhibited stability for 30 h.

In a recent study by Lan et al. [175], the Ni-to-Fe ratio was examined in catalysts prepared under an external magnetic field. The catalyst with the highest performance for CO_2 methanation had a Ni-to-Fe ratio of 8/2 (Ni8Fe2). This particular catalyst achieved a conversion rate of over 80% of CO_2 into CH_4 at 150 °C, along with a CH_4 selectivity of 95% under controlled reaction conditions, including a GHSV of 10,000 (mL.g^{-1}h^{-1}) and 1 atm. Furthermore, the Ni8Fe2 catalyst maintained stable activity for 200 h.

The addition of Fe increases the surface area and reduces the size of Ni crystals. Consequently, Fe-promoted catalysts exhibit improved CO_2 conversion and CH_4 selectivity compared with unpromoted catalysts. Notably, these catalysts also show enhanced resistance to carbon formation. However, it is important to note that further research is needed to fully understand the synergistic effects of Ni and Fe in these catalysts and to elucidate the underlying reaction mechanisms over Fe-based catalysts.

4.3. Summary of Performance of Non-Noble Catalysts

Non-noble catalysts for CO_2 methanation include Ni-, Co-, and Fe-based catalysts; among all catalyst systems, Ni-based catalysts show the best catalytic performance. The selectivity to CH_4 is generally high (close to 100%), especially at low reaction temperatures (lower than 400 °C), and they have revealed very good activity. Excellent Ni-based catalysts can reach or come close to equilibrium conversion at around 350 °C and 1 atm with a WHSV of 10,000 mL.g^{-1}h^{-1} or even higher, and the stability generally extends to several hundred hours. For Co- and Fe-based catalysts, some show very high activity at low temperatures, though the stability and selectivity compared with the corresponding catalyst is possibly not good enough. Co- and Fe-based catalysts are well known for being used as FTS catalysts, which means that hydrocarbons besides CH_4 can be easily generated, thus leading to decreased selectivity to CH_4.

In this study, the catalytic performance of noble metal catalysts was found to be dependent on metal dispersion, metal–support interactions, and additive doping. Various catalyst configurations, including supports made of single-oxide supports (Al_2O_3, TiO_2, ZrO_2, and CeO_2), composite oxide supports (Ce-Zr-O), basic oxide promoters, and bimetallic systems, were investigated to determine their impact on catalytic activity and stability. These results suggest that Ni-based catalysts are the most promising.

The development of an industrially viable catalyst for CO_2 methanation requires rigorous evaluations of its activity, selectivity, and stability. Achieving 100% CO_2 conversion to CH_4, maintaining stability for extended periods (3–4 years), and operating under typical industrial pressures (2–5 MPa) are crucial goals. To assess catalyst performance, we connected experimental data from the literature, presented in Tables 2 and 3, and corresponding explanations are provided above. For noble metal catalysts, Ru-based catalysts are the best; the activity and selectivity are very good, but the stability lasts only for 300 h in the most stable catalyst. The critical obstacle for industrial application would be the high price and high noble metal loading in these catalysts. For non-noble metal catalysts, Ni-based catalysts are the best; the activity and selectivity are also very good, and as for

stability, many studies have shown that stability lasts for 100 to 400 h. It seems that the stability of Ni-based catalysts is promising.

It should be noted that carbon deposition for CO_2 methanation is rare; it is likely that carbon deposition for CO_2 methanation is not severe because CO_2 can eliminate the deposited carbon by reacting with the carbon to produce CO and H_2.

To develop a catalyst for industrial applications of CO_2 methanation, investigations of the following are necessary: (1) A study of catalytic performance under industrial conditions is necessary at pressures from 2.0 to 6.0 MPa, reaction temperatures between 250 and 600 °C, and various space velocities; specific reaction conditions depend on the particular industrial situation. The reported literature primarily conducts experiments at 1 atm; an increased reaction temperature favors a decrease in the number of molecules reacting with CO_2, which may not always be true, as pressure also affects the adsorption and activation of both the targeted reaction and the byproducts' reactions. (2) An investigation of stability over much longer periods is needed; the stability of the CO_2 methanation reaction has only been studied for hundreds of hours in the literature, whereas an industrial catalyst should be stable for years. (3) The improvement of activity at low reaction temperatures is essential. As can be seen from the thermodynamic equilibrium profile in Figure 2b, the complete conversion of CO_2 into CH_4 is achievable only at low temperatures and comparatively high pressures; therefore, high activity at low temperatures is required.

5. Conclusions and Future Prospective

In combatting the challenges posed by CO_2 emissions, using renewable energy to produce green hydrogen and then hydrogenating CO_2 into valuable chemicals is a promising route, including through the production of CH_4 via CO_2 methanation. Given the thermodynamic equilibrium of the reaction, to convert CO_2 completely into CH_4, low reaction temperatures and high pressure are favorable, and meeting the requirements of developing catalysts is critical. The catalysts that have been extensively reported include noble metal-based catalysts and non-noble metal-based catalysts.

Among the noble metal catalysts, Ru shows the best catalytic performance. In excellent Ru-based catalysts, CO_2 conversion can be achieved close to equilibrium (98%) and with 100% selectivity to CH_4, with 300 h of stability obtained at 24,000 $mL.g^{-1}h^{-1}$, 230 °C, and 1 atm. Excellent noble metal-based catalysts feature the high dispersion of the noble metal, the strong metal-support interaction with noble metal NPs, and doped with a transitional metal: Ni, Co, or Fe. The disadvantages of noble metal-based catalysts are the high price and high loading, and the stability needs to be improved.

Non-noble metal catalysts include Ni-, Co-, and Fe-based catalysts. Ni-based catalysts show the best catalytic performance and are well studied, while studies on Co- and Fe-based catalysts are much fewer, possibly because other hydrocarbons besides CH_4 can be formed over Co and Fe catalysts. With excellent Ni-based catalysts, CO_2 conversion close to equilibrium (around 90%) and 100% selectivity to CH_4 can be obtained at around 350 °C a WHSV of 10,000 ($mL.g^{-1}h^{-1}$) or higher, and 1 atm with good stability. Excellent Ni-based catalysts feature high Ni NP dispersion; a support and/or additive to activate or help activate CO_2; and interactions between Ni NPs and the support that resist sintering. Bimetals (Ni-Fe, Ni-Co) are favorable for improving catalytic performance.

Author Contributions: Conceptualization, M.A.M.; methodology, M.A.M., Y.J. and M.A.; writing—original draft preparation, M.A.M.; writing—review and editing, M.A.M., M.A. and M.A.H.; visualization, M.A.H.; supervision, H.W. and Y.L. All authors have read and agreed to the published version of the manuscript.

Funding: Financial support for this work from the National Natural Science Foundation of China (Nos. 21872101, 21962014).

Data Availability Statement: Data is contained within the article.

Conflicts of Interest: The authors declare no conflict of interest.

References

1. Ahn, J.; Chung, W. A Study on Activity of Coexistent CO Gas during the CO_2 Methanation Reaction in Ni-Based Catalyst. *Processes* **2023**, *11*, 628. [CrossRef]
2. Asim, M.; Maryam, B.; Zhang, S.; Sajid, M.; Kurbanov, A.; Pan, L.; Zou, J.J. Synergetic effect of Au nanoparticles and transition metal phosphides for enhanced hydrogen evolution from ammonia-borane. *J. Colloid Interface Sci.* **2023**, *638*, 14–25. [CrossRef] [PubMed]
3. Mebrahtu, C.; Krebs, F.; Abate, S.; Perathoner, S.; Centi, G.; Palkovits, R. *CO_2 Methanation: Principles and Challenges*, 1st ed.; Elsevier B.V.: Amsterdam, The Netherlands, 2019; Volume 178, ISBN 9780444641274.
4. Asim, M.; Zhang, S.; Maryam, B.; Xiao, J.; Shi, C.; Pan, L.; Zou, J.J. Pt loading to promote hydrogen evolution from ammonia-borane hydrolysis of Ni2P under visible light. *Appl. Surf. Sci.* **2023**, *620*, 156787. [CrossRef]
5. Hassan, M.A.; Mehmood, T.; Liu, J.; Luo, X.; Li, X.; Tanveer, M.; Faheem, M.; Shakoor, A.; Dar, A.A.; Abid, M. A review of particulate pollution over Himalaya region: Characteristics and salient factors contributing ambient PM pollution. *Atmos. Environ.* **2023**, *294*, 119472. [CrossRef]
6. Mehmood, T.; Hassan, M.A.; Li, X.; Ashraf, A.; Rehman, S.; Bilal, M.; Obodo, R.M.; Mustafa, B.; Shaz, M.; Bibi, S. Mechanism behind sources and sinks of major anthropogenic greenhouse gases. In *Climate Change Alleviation for Sustainable Progression*; CRC Press: Boca Raton, FL, USA, 2022; pp. 114–150.
7. Bai, C.; Chen, Z.; Wang, D. Transportation carbon emission reduction potential and mitigation strategy in China. *Sci. Total Environ.* **2023**, *873*, 162074. [CrossRef]
8. Zhu, Q. Developments on CO_2-utilization technologies. *Clean Energy* **2019**, *3*, 85–100. [CrossRef]
9. Petrovic, B.; Gorbounov, M.; Masoudi Soltani, S. Influence of surface modification on selective CO_2 adsorption: A technical review on mechanisms and methods. *Microporous Mesoporous Mater.* **2021**, *312*, 110751. [CrossRef]
10. IPCC. *Summary for Policymakers Sixth Assessment Report (WG3)*; IPCC: Geneva, Switzerland, 2022; ISBN 9781107415416.
11. Hassan, M.A.; Mehmood, T.; Lodhi, E.; Bilal, M.; Dar, A.A.; Liu, J. Lockdown Amid COVID-19 Ascendancy over Ambient Particulate Matter Pollution Anomaly. *Int. J. Environ. Res. Public Health* **2022**, *19*, 3540. [CrossRef]
12. Hassan, M.A.; Faheem, M.; Mehmood, T.; Yin, Y.; Liu, J. Assessment of meteorological and air quality drivers of elevated ambient ozone in Beijing via machine learning approach. *Environ. Sci. Pollut. Res.* **2023**, *30*, 104086–104099. [CrossRef] [PubMed]
13. Mustafa, A.; Lougou, B.G.; Shuai, Y.; Wang, Z.; Tan, H. Current technology development for CO_2 utilization into solar fuels and chemicals: A review. *J. Energy Chem.* **2020**, *49*, 96–123. [CrossRef]
14. Dlugokencky, E.; Tans, P. Co2_Trend_Gl.Pdf. Available online: https://www.esrl.noaa.gov/gmd/ccgg/trends/global.html (accessed on 5 November 2023).
15. Warsi, Y.; Kabanov, V.; Zhou, P.; Sinha, A. Novel Carbon Dioxide Utilization Technologies: A Means to an End. *Front. Energy Res.* **2020**, *8*, 574147. [CrossRef]
16. Raheem, I.; Mubarak, N.M.; Karri, R.R.; Manoj, T.; Ibrahim, S.M.; Mazari, S.A.; Nizamuddin, S. Forecasting of energy consumption by G20 countries using an adjacent accumulation grey model. *Sci. Rep.* **2022**, *12*, 13417. [CrossRef]
17. World Meteorological Organization (WMO). *WMO Global Annual to Decadal Climate Update*; World Meteorological Organization (WMO): Geneva, Switzerland, 2023.
18. Monthly Average Mauna Loa CO_2 Monthly Average Mauna Loa CO_2.pdf. Available online: https://www.gml.noaa.gov/ccgg/trends/ (accessed on 21 November 2022).
19. Khdary, N.H.; Alayyar, A.S.; Alsarhan, L.M.; Alshihri, S.; Mokhtar, M. Metal Oxides as Catalyst/Supporter for CO_2 Capture and Conversion, Review. *Catalysts* **2022**, *12*, 300. [CrossRef]
20. UNFCCC. *UN Climate Change ANNUAL REPORT 2017*; United Nations Framework Convention on Climate Change: Bonn, Germany, 2017; ISBN 9789292191757.
21. Rafiee, A.; Rajab Khalilpour, K.; Milani, D.; Panahi, M. Trends in CO_2 conversion and utilization: A review from process systems perspective. *J. Environ. Chem. Eng.* **2018**, *6*, 5771–5794. [CrossRef]
22. Saravanan, A.; Senthil kumar, P.; Vo, D.V.N.; Jeevanantham, S.; Bhuvaneswari, V.; Anantha Narayanan, V.; Yaashikaa, P.R.; Swetha, S.; Reshma, B. A comprehensive review on different approaches for CO_2 utilization and conversion pathways. *Chem. Eng. Sci.* **2021**, *236*, 116515. [CrossRef]
23. Feng, X.; Wang, K.; Zhou, M.; Li, F.; Liu, J.; Zhao, M.; Zhao, L.; Song, X.; Zhang, P.; Gao, L. Metal organic framework derived Ni/CeO_2 catalyst with highly dispersed ultra-fine Ni nanoparticles: Impregnation synthesis and the application in CO_2 methanation. *Ceram. Int.* **2021**, *47*, 12366–12374. [CrossRef]
24. Takht Ravanchi, M.; Sahebdelfar, S. Catalytic conversions of CO_2 to help mitigate climate change: Recent process developments. *Process Saf. Environ. Prot.* **2021**, *145*, 172–194. [CrossRef]
25. Liu, M.; Yi, Y.; Wang, L.; Guo, H.; Bogaerts, A. Hydrogenation of carbon dioxide to value-added chemicals by heterogeneous catalysis and plasma catalysis. *Catalysts* **2019**, *9*, 275. [CrossRef]
26. Asim, M.; Zhang, S.; Wang, Y.; Maryam, B.; Sajid, M.; Shi, C.; Pan, L.; Zhang, X.; Zou, J.J. Self-supporting NiCoP for hydrogen generation via hydrolysis of ammonia borane. *Fuel* **2022**, *318*, 123544. [CrossRef]
27. Garba, M.D.; Usman, M.; Khan, S.; Shehzad, F.; Galadima, A.; Ehsan, M.F.; Ghanem, A.S.; Humayun, M. CO_2 towards fuels: A review of catalytic conversion of carbon dioxide to hydrocarbons. *J. Environ. Chem. Eng.* **2021**, *9*, 104756. [CrossRef]

28. Italiano, C.; Llorca, J.; Pino, L.; Ferraro, M.; Antonucci, V.; Vita, A. CO and CO_2 methanation over Ni catalysts supported on CeO_2, Al_2O_3 and Y_2O_3 oxides. *Appl. Catal. B Environ.* **2020**, *264*, 118494. [CrossRef]
29. Varvoutis, G.; Lampropoulos, A.; Oikonomou, P.; Andreouli, C.D.; Stathopoulos, V.; Lykaki, M.; Marnellos, G.E.; Konsolakis, M. Fabrication of highly active and stable Ni/CeO_2-nanorods wash-coated on ceramic NZP structured catalysts for scaled-up CO_2 methanation. *J. CO2 Util.* **2023**, *70*, 102425. [CrossRef]
30. Varvoutis, G.; Karakoulia, S.A.; Lykaki, M.; Stefa, S.; Binas, V.; Marnellos, G.E.; Konsolakis, M. Support-induced modifications on the CO_2 hydrogenation performance of Ni/CeO_2: The effect of ZnO doping on CeO_2 nanorods. *J. CO2 Util.* **2022**, *61*, 102057. [CrossRef]
31. Refaat, Z.; El Saied, M.; El Naga, A.O.A.; Shaban, S.A.; Hassan, H.B.; Shehata, M.R.; Kady, F.Y.E. Efficient CO_2 methanation using nickel nanoparticles supported mesoporous carbon nitride catalysts. *Sci. Rep.* **2023**, *13*, 4855. [CrossRef] [PubMed]
32. Gholami, S.; Alavi, S.M.; Rezaei, M. Preparation of highly active and stable nanostructured Ni-Cr_2O_3 catalysts for hydrogen purification via CO_2 methanation reaction. *J. Energy Inst.* **2021**, *95*, 132–142. [CrossRef]
33. Zhou, G.; Wu, T.; Xie, H.; Zheng, X. Effects of structure on the carbon dioxide methanation performance of Co-based catalysts. *Int. J. Hydrogen Energy* **2013**, *38*, 10012–10018. [CrossRef]
34. Nieß, S.; Armbruster, U.; Dietrich, S.; Klemm, M. Recent Advances in Catalysis for Methanation of CO_2 from Biogas. *Catalysts* **2022**, *12*, 374. [CrossRef]
35. Cárdenas-Arenas, A.; Quindimil, A.; Davó-Quiñonero, A.; Bailón-García, E.; Lozano-Castelló, D.; De-La-Torre, U.; Pereda-Ayo, B.; González-Marcos, J.A.; González-Velasco, J.R.; Bueno-López, A. Isotopic and in situ DRIFTS study of the CO_2 methanation mechanism using Ni/CeO_2 and Ni/Al_2O_3 catalysts. *Appl. Catal. B Environ.* **2020**, *265*, 118538. [CrossRef]
36. Gao, J.; Liu, Q.; Gu, F.; Liu, B.; Zhong, Z.; Su, F. Recent advances in methanation catalysts for the production of synthetic natural gas. *RSC Adv.* **2015**, *5*, 22759–22776. [CrossRef]
37. Aldana, P.A.U.; Ocampo, F.; Kobl, K.; Louis, B.; Thibault-Starzyk, F.; Daturi, M.; Bazin, P.; Thomas, S.; Roger, A.C. Catalytic CO_2 valorization into CH_4 on Ni-based ceria-zirconia. Reaction mechanism by operando IR spectroscopy. *Catal. Today* **2013**, *215*, 201–207. [CrossRef]
38. Wang, S.; Pan, Q.; Peng, J.; Wang, S. In situ FTIR spectroscopic study of the CO_2 methanation mechanism on Ni/$Ce_{0.5}Zr_{0.5}O_2$. *Catal. Sci. Technol.* **2014**, *4*, 502–509. [CrossRef]
39. Akamaru, S.; Shimazaki, T.; Kubo, M.; Abe, T. Density functional theory analysis of methanation reaction of CO_2 on Ru nanoparticle supported on TiO_2 (1 0 1). *Appl. Catal. A Gen.* **2014**, *470*, 405–411. [CrossRef]
40. Miao, B.; Ma, S.S.K.; Wang, X.; Su, H.; Chan, S.H. Catalysis mechanisms of CO_2 and CO methanation. *Catal. Sci. Technol.* **2016**, *6*, 4048–4058. [CrossRef]
41. Xu, X.; Tong, Y.; Huang, J.; Zhu, J.; Fang, X.; Xu, J.; Wang, X. Insights into CO_2 methanation mechanism on cubic ZrO_2 supported Ni catalyst via a combination of experiments and DFT calculations. *Fuel* **2021**, *283*, 118867. [CrossRef]
42. Su, X.; Xu, J.; Liang, B.; Duan, H.; Hou, B.; Huang, Y. Catalytic carbon dioxide hydrogenation to methane: A review of recent studies. *J. Energy Chem.* **2016**, *25*, 553–565. [CrossRef]
43. Zhang, J.; Yang, Y.; Liu, J.; Xiong, B. Mechanistic understanding of CO_2 hydrogenation to methane over Ni/CeO_2 catalyst. *Appl. Surf. Sci.* **2021**, *558*, 149866. [CrossRef]
44. Ren, J.; Guo, H.; Yang, J.; Qin, Z.; Lin, J.; Li, Z. Insights into the mechanisms of CO_2 methanation on Ni(111) surfaces by density functional theory. *Appl. Surf. Sci.* **2015**, *351*, 504–516. [CrossRef]
45. Jia, X.; Zhang, X.; Rui, N.; Hu, X.; Liu, C.j. Structural effect of Ni/ZrO_2 catalyst on CO_2 methanation with enhanced activity. *Appl. Catal. B Environ.* **2019**, *244*, 159–169. [CrossRef]
46. Gao, J.; Wang, Y.; Ping, Y.; Hu, D.; Xu, G.; Gu, F.; Su, F. A thermodynamic analysis of methanation reactions of carbon oxides for the production of synthetic natural gas. *RSC Adv.* **2012**, *2*, 2358–2368. [CrossRef]
47. Pan, Q.; Peng, J.; Sun, T.; Wang, S.; Wang, S. Insight into the reaction route of CO_2 methanation: Promotion effect of medium basic sites. *Catal. Commun.* **2014**, *45*, 74–78. [CrossRef]
48. Ridzuan, N.D.M.; Shaharun, M.S.; Anawar, M.A.; Ud-Din, I. Ni-Based Catalyst for Carbon Dioxide Methanation: A Review. *Catalysts* **2022**, *12*, 469. [CrossRef]
49. Lee, W.J.; Li, C.; Prajitno, H.; Yoo, J.; Patel, J.; Yang, Y.; Lim, S. Recent trend in thermal catalytic low temperature CO_2 methanation: A critical review. *Catal. Today* **2021**, *368*, 2–19. [CrossRef]
50. Martínez, J.; Hernández, E.; Alfaro, S.; Medina, R.L.; Aguilar, G.V.; Albiter, E.; Valenzuela, M.A. High selectivity and stability of nickel catalysts for CO_2 Methanation: Support effects. *Catalysts* **2019**, *9*, 24. [CrossRef]
51. Liang, C.; Zhang, L.; Zheng, Y.; Zhang, S.; Liu, Q.; Gao, G.; Dong, D.; Wang, Y.; Xu, L.; Hu, X. Methanation of CO_2 over nickel catalysts: Impacts of acidic/basic sites on formation of the reaction intermediates. *Fuel* **2020**, *262*, 116521. [CrossRef]
52. Razzaq, R.; Zhu, H.; Jiang, L.; Muhammad, U.; Li, C.; Zhang, S. Catalytic methanation of CO and CO_2 in coke oven gas over Ni-Co/ZrO_2-CeO_2. *Ind. Eng. Chem. Res.* **2013**, *52*, 2247–2256. [CrossRef]
53. Li, S.; Tang, H.; Gong, D.; Ma, Z.; Liu, Y. Loading Ni/La_2O_3 on SiO_2 for CO methanation from syngas. *Catal. Today* **2017**, *297*, 298–307. [CrossRef]
54. Stangeland, K.; Kalai, D.; Li, H.; Yu, Z. CO_2 Methanation: The Effect of Catalysts and Reaction Conditions. *Energy Procedia* **2017**, *105*, 2022–2027. [CrossRef]

55. Brooks, K.P.; Hu, J.; Zhu, H.; Kee, R.J. Methanation of carbon dioxide by hydrogen reduction using the Sabatier process in microchannel reactors. *Chem. Eng. Sci.* **2007**, *62*, 1161–1170. [CrossRef]
56. Jürgensen, L.; Ehimen, E.A.; Born, J.; Holm-Nielsen, J.B. Dynamic biogas upgrading based on the Sabatier process: Thermodynamic and dynamic process simulation. *Bioresour. Technol.* **2015**, *178*, 323–329. [CrossRef] [PubMed]
57. Yarbaş, T.; Ayas, N. A detailed thermodynamic analysis of CO_2 hydrogenation to produce methane at low pressure. *Int. J. Hydrogen Energy* **2023**, *49*, 1134–1144. [CrossRef]
58. Hofmann, A. *Physical Chemistry Essentials*; Springer: Cham, Switzerland, 2018; ISBN 9783319741673.
59. Abdel-Mageed, A.M.; Wohlrab, S. Review of CO_2 reduction on supported metals (Alloys) and single-atom catalysts (SACs) for the use of green hydrogen in power-to-gas concepts. *Catalysts* **2022**, *12*, 16. [CrossRef]
60. Sharifian, S.; Asasian-Kolur, N. Studies on COx hydrogenation to methane over Rh-based catalysts. *Inorg. Chem. Commun.* **2020**, *118*, 108021. [CrossRef]
61. Kuznecova, I.; Gusca, J. Property based ranking of CO and CO_2 methanation catalysts. *Energy Procedia* **2017**, *128*, 255–260. [CrossRef]
62. Garbarino, G.; Bellotti, D.; Riani, P.; Magistri, L.; Busca, G. Methanation of carbon dioxide on Ru/Al_2O_3 and Ni/Al_2O_3 catalysts at atmospheric pressure: Catalysts activation, behaviour and stability. *Int. J. Hydrogen Energy* **2015**, *40*, 9171–9182. [CrossRef]
63. Park, S.J.; Wang, X.; Ball, M.R.; Proano, L.; Wu, Z.; Jones, C.W. CO_2 methanation reaction pathways over unpromoted and $NaNO_3$-promoted Ru/Al_2O_3 catalysts. *Catal. Sci. Technol.* **2022**, *12*, 4637–4652. [CrossRef]
64. Tada, S.; Shimizu, T.; Kameyama, H.; Haneda, T.; Kikuchi, R. Ni/CeO_2 catalysts with high CO_2 methanation activity and high CH_4 selectivity at low temperatures. *Int. J. Hydrogen Energy* **2012**, *37*, 5527–5531. [CrossRef]
65. Aitbekova, A.; Wu, L.; Wrasman, C.J.; Boubnov, A.; Hoffman, A.S.; Goodman, E.D.; Bare, S.R.; Cargnello, M. Low-Temperature Restructuring of CeO_2-Supported Ru Nanoparticles Determines Selectivity in CO_2 Catalytic Reduction. *J. Am. Chem. Soc.* **2018**, *140*, 13736–13745. [CrossRef] [PubMed]
66. Abe, T.; Tanizawa, M.; Watanabe, K.; Taguchi, A. CO_2 methanation property of Ru nanoparticle-loaded TiO_2 prepared by a polygonal barrel-sputtering method. *Energy Environ. Sci.* **2009**, *2*, 315–321. [CrossRef]
67. Hatzisymeon, M.; Petala, A.; Panagiotopoulou, P. Carbon Dioxide Hydrogenation over Supported Ni and Ru Catalysts. *Catal. Lett.* **2021**, *151*, 888–900. [CrossRef]
68. Martinez T, L.M.; Muñoz, A.; Pérez, A.; Laguna, O.H.; Bobadilla, L.F.; Centeno, M.A.; Odriozola, J.A. The effect of support surface hydroxyls on selective CO methanation with Ru based catalysts. *Appl. Catal. A Gen.* **2022**, *641*, 118678. [CrossRef]
69. Loccufier, E.; Watson, G.; Zhao, Y.; Meledina, M.; Denis, R.; Derakhshandeh, P.G.; Van Der Voort, P.; Leus, K.; Debecker, D.P.; De Buysser, K.; et al. CO_2 methanation with Ru@MIL-101 nanoparticles fixated on silica nanofibrous veils as stand-alone structured catalytic carrier. *Appl. Catal. B Environ.* **2023**, *320*, 121972. [CrossRef]
70. Bobadilla, L.F.; Muñoz-Murillo, A.; Laguna, O.H.; Centeno, M.A.; Odriozola, J.A. Does shaping catalysts modify active phase sites? A comprehensive in situ FTIR spectroscopic study on the performance of a model Ru/Al_2O_3 catalyst for the CO methanation. *Chem. Eng. J.* **2019**, *357*, 248–257. [CrossRef]
71. Fechete, I.; Vedrine, J.C. Nanoporous materials as new engineered catalysts for the synthesis of green fuels. *Molecules* **2015**, *20*, 5638–5666. [CrossRef] [PubMed]
72. Wang, C.; Lu, Y.; Zhang, Y.; Fu, H.; Sun, S.; Li, F.; Duan, Z.; Liu, Z.; Wu, C.; Wang, Y.; et al. Ru-based catalysts for efficient CO_2 methanation: Synergistic catalysis between oxygen vacancies and basic sites. *Nano Res.* **2023**, *16*, 12153–12164. [CrossRef]
73. Shang, X.; Deng, D.; Wang, X.; Xuan, W.; Zou, X.; Ding, W.; Lu, X. Enhanced low-temperature activity for CO_2 methanation over Ru doped the $Ni/CexZr_{(1-x)}O_2$ catalysts prepared by one-pot hydrolysis method. *Int. J. Hydrogen Energy* **2018**, *43*, 7179–7189. [CrossRef]
74. Tada, S.; Ochieng, O.J.; Kikuchi, R.; Haneda, T.; Kameyama, H. Promotion of CO_2 methanation activity and CH_4 selectivity at low temperatures over $Ru/CeO_2/Al_2O_3$ catalysts. *Int. J. Hydrogen Energy* **2014**, *39*, 10090–10100. [CrossRef]
75. Chai, S.; Men, Y.; Wang, J.; Liu, S.; Song, Q.; An, W.; Kolb, G. Boosting CO_2 methanation activity on Ru/TiO_2 catalysts by exposing (001) facets of anatase TiO_2. *J. CO2 Util.* **2019**, *33*, 242–252. [CrossRef]
76. Lippi, R.; Howard, S.C.; Barron, H.; Easton, C.D.; Madsen, I.C.; Waddington, L.J.; Vogt, C.; Hill, M.R.; Sumby, C.J.; Doonan, C.J.; et al. Highly active catalyst for CO_2 methanation derived from a metal organic framework template. *J. Mater. Chem. A* **2017**, *5*, 12990–12997. [CrossRef]
77. Sakpal, T.; Lefferts, L. Structure-dependent activity of CeO_2 supported Ru catalysts for CO_2 methanation. *J. Catal.* **2018**, *367*, 171–180. [CrossRef]
78. Dreyer, J.A.H.; Li, P.; Zhang, L.; Beh, G.K.; Zhang, R.; Sit, P.H.L.; Teoh, W.Y. Influence of the oxide support reducibility on the CO_2 methanation over Ru-based catalysts. *Appl. Catal. B Environ.* **2017**, *219*, 715–726. [CrossRef]
79. Jiang, Y.; Lang, J.; Wu, X.; Hu, Y.H. Electronic structure modulating for supported Rh catalysts toward CO_2 methanation. *Catal. Today* **2020**, *356*, 570–578. [CrossRef]
80. Ocampo, F.; Louis, B.; Kiwi-Minsker, L.; Roger, A.C. Effect of Ce/Zr composition and noble metal promotion on nickel based $Ce_xZr_{1-x}O_2$ catalysts for carbon dioxide methanation. *Appl. Catal. A Gen.* **2011**, *392*, 36–44. [CrossRef]
81. Bando, K.K.; Soga, K.; Kunimori, K.; Ichikuni, N.; Okabe, K.; Kusama, H.; Sayama, K.; Arakawa, H. CO_2 hydrogenation activity and surface structure of zeolite-supported Rh catalysts. *Appl. Catal. A Gen.* **1998**, *173*, 47–60. [CrossRef]

82. Martin, N.M.; Hemmingsson, F.; Schaefer, A.; Ek, M.; Merte, L.R.; Hejral, U.; Gustafson, J.; Skoglundh, M.; Dippel, A.C.; Gutowski, O.; et al. Structure-function relationship for CO_2 methanation over ceria supported Rh and Ni catalysts under atmospheric pressure conditions. *Catal. Sci. Technol.* **2019**, *9*, 1644–1653. [CrossRef]
83. Younas, M.; Sethupathi, S.; Kong, L.L.; Mohamed, A.R. CO_2 methanation over Ni and Rh based catalysts: Process optimization at moderate temperature. *Int. J. Energy Res.* **2018**, *42*, 3289–3302. [CrossRef]
84. Bakar, W.A.W.A.; Ali, R.; Toemen, S. Catalytic methanation reaction over supported nickel-rhodium oxide for purification of simulated natural gas. *J. Nat. Gas Chem.* **2011**, *20*, 585–594. [CrossRef]
85. Meloni, E.; Cafiero, L.; Renda, S.; Martino, M.; Pierro, M. Ru- and Rh-Based Catalysts for CO_2 Methanation Assisted by Non-Thermal Plasma. *Catalysts* **2023**, *13*, 488. [CrossRef]
86. Mihet, M.; Lazar, M.D. Methanation of CO_2 on Ni/γ-Al_2O_3: Influence of Pt, Pd or Rh promotion. *Catal. Today* **2018**, *306*, 294–299. [CrossRef]
87. Jiang, H.; Gao, Q.; Wang, S.; Chen, Y.; Zhang, M. The synergistic effect of Pd NPs and UiO-66 for enhanced activity of carbon dioxide methanation. *J. CO2 Util.* **2019**, *31*, 167–172. [CrossRef]
88. Wang, X.; Shi, H.; Kwak, J.H.; Szanyi, J. Mechanism of CO_2 Hydrogenation on Pd/Al_2O_3 Catalysts: Kinetics and Transient DRIFTS-MS Studies. *ACS Catal.* **2015**, *5*, 6337–6349. [CrossRef]
89. Wang, K.; Li, W.; Huang, J.; Huang, J.; Zhan, G.; Li, Q. Enhanced active site extraction from perovskite $LaCoO_3$ using encapsulated PdO for efficient CO_2 methanation. *J. Energy Chem.* **2020**, *53*, 9–19. [CrossRef]
90. Park, J.N.; McFarland, E.W. A highly dispersed Pd-Mg/SiO_2 catalyst active for methanation of CO_2. *J. Catal.* **2009**, *266*, 92–97. [CrossRef]
91. Luo, L.; Wang, M.; Cui, Y.; Chen, Z.; Wu, J.; Cao, Y.; Luo, J.; Dai, Y.; Li, W.X.; Bao, J.; et al. Surface Iron Species in Palladium–Iron Intermetallic Nanocrystals that Promote and Stabilize CO_2 Methanation. *Angew. Chem.-Int. Ed.* **2020**, *59*, 14434–14442. [CrossRef] [PubMed]
92. Frontera, P.; Macario, A.; Ferraro, M.; Antonucci, P.L. Supported catalysts for CO_2 methanation: A review. *Catalysts* **2017**, *7*, 59. [CrossRef]
93. Karelovic, A.; Ruiz, P. Improving the hydrogenation function of Pd/γ-Al_2O_3 catalyst by Rh/γ-Al_2O_3 Addition in CO_2 methanation at low temperature. *ACS Catal.* **2013**, *3*, 2799–2812. [CrossRef]
94. Arandiyan, H.; Kani, K.; Wang, Y.; Jiang, B.; Kim, J.; Yoshino, M.; Rezaei, M.; Rowan, A.E.; Dai, H.; Yamauchi, Y. Highly Selective Reduction of Carbon Dioxide to Methane on Novel Mesoporous Rh Catalysts. *ACS Appl. Mater. Interfaces* **2018**, *10*, 24963–24968. [CrossRef]
95. Debek, R. Novel Catalysts for Chemical CO_2 Utilization. Doctoral Dissertation, Université Pierre et Marie Curie, Paris, France, AGH University of Science and Technology, Kraków, Poland, 2016; pp. 1–257.
96. Dębek, R.; Azzolina-Jury, F.; Travert, A.; Maugé, F. A review on plasma-catalytic methanation of carbon dioxide—Looking for an efficient catalyst. *Renew. Sustain. Energy Rev.* **2019**, *116*, 109427. [CrossRef]
97. Haneda, M.; Shinoda, K.; Nagane, A.; Houshito, O.; Takagi, H.; Nakahara, Y.; Hiroe, K.; Fujitani, T.; Hamada, H. Catalytic performance of rhodium supported on ceria-zirconia mixed oxides for reduction of NO by propene. *J. Catal.* **2008**, *259*, 223–231. [CrossRef]
98. Phatak, A.A.; Koryabkina, N.; Rai, S.; Ratts, J.L.; Ruettinger, W.; Farrauto, R.J.; Blau, G.E.; Delgass, W.N.; Ribeiro, F.H. Kinetics of the water-gas shift reaction on Pt catalysts supported on alumina and ceria. *Catal. Today* **2007**, *123*, 224–234. [CrossRef]
99. Hu, D.; Gao, J.; Ping, Y.; Jia, L.; Gunawan, P.; Zhong, Z.; Xu, G.; Gu, F.; Su, F. Enhanced investigation of CO methanation over Ni/Al_2O_3 catalysts for synthetic natural gas production. *Ind. Eng. Chem. Res.* **2012**, *51*, 4875–4886. [CrossRef]
100. Lee, S.M.; Lee, Y.H.; Moon, D.H.; Ahn, J.Y.; Nguyen, D.D.; Chang, S.W.; Kim, S.S. Reaction Mechanism and Catalytic Impact of Ni/CeO_{2-x} Catalyst for Low-Temperature CO_2 Methanation. *Ind. Eng. Chem. Res.* **2019**, *58*, 8656–8662. [CrossRef]
101. Wu, H.C.; Chen, T.C.; Wu, J.H.; Pao, C.W.; Chen, C.S. Influence of sodium-modified Ni/SiO_2 catalysts on the tunable selectivity of CO_2 hydrogenation: Effect of the CH_4 selectivity, reaction pathway and mechanism on the catalytic reaction. *J. Colloid Interface Sci.* **2021**, *586*, 514–527. [CrossRef] [PubMed]
102. Yan, Z.; Liu, Q.; Liang, L.; Ouyang, J. Surface hydroxyls mediated CO_2 methanation at ambient pressure over attapulgite-loaded Ni-TiO_2composite catalysts with high activity and reuse ability. *J. CO2 Util.* **2021**, *47*, 101489. [CrossRef]
103. Zhou, R.; Rui, N.; Fan, Z.; Liu, C. jun Effect of the structure of Ni/TiO_2 catalyst on CO_2 methanation. *Int. J. Hydrogen Energy* **2016**, *41*, 22017–22025. [CrossRef]
104. Zeng, L.; Wang, Y.; Li, Z.; Song, Y.; Zhang, J.; Wang, J.; He, X.; Wang, C.; Lin, W. Highly Dispersed Ni Catalyst on Metal-Organic Framework-Derived Porous Hydrous Zirconia for CO_2 Methanation. *ACS Appl. Mater. Interfaces* **2020**, *12*, 17436–17442. [CrossRef] [PubMed]
105. Foraita, S.; Fulton, J.L.; Chase, Z.A.; Vjunov, A.; Xu, P.; Baráth, E.; Camaioni, D.M.; Zhao, C.; Lercher, J.A. Impact of the oxygen defects and the hydrogen concentration on the surface of tetragonal and monoclinic ZrO_2 on the reduction rates of stearic acid on Ni/ZrO_2. *Chem.-A Eur. J.* **2015**, *21*, 2423–2434. [CrossRef] [PubMed]
106. Ratchahat, S.; Sudoh, M.; Suzuki, Y.; Kawasaki, W.; Watanabe, R.; Fukuhara, C. Development of a powerful CO_2 methanation process using a structured Ni/CeO_2 catalyst. *J. CO2 Util.* **2018**, *24*, 210–219. [CrossRef]
107. Zhou, G.; Liu, H.; Cui, K.; Jia, A.; Hu, G.; Jiao, Z.; Liu, Y.; Zhang, X. Role of surface Ni and Ce species of Ni/CeO_2 catalyst in CO_2 methanation. *Appl. Surf. Sci.* **2016**, *383*, 248–252. [CrossRef]

108. Sun, H.; Wang, H.; Liu, X.; Zhang, Z.; Zhang, S.; Wang, X.; Liu, Y. Stable and Highly Dispersed Nickel Catalysts on Ce-Zr-O Solid Solutions for CO_2 Methanation. *ChemistrySelect* **2022**, *7*, 2–10. [CrossRef]
109. Takano, H.; Kirihata, Y.; Izumiya, K.; Kumagai, N.; Habazaki, H.; Hashimoto, K. Highly active Ni/Y-doped ZrO_2 catalysts for CO_2 methanation. *Appl. Surf. Sci.* **2016**, *388*, 653–663. [CrossRef]
110. Muroyama, H.; Tsuda, Y.; Asakoshi, T.; Masitah, H.; Okanishi, T.; Matsui, T.; Eguchi, K. Carbon dioxide methanation over Ni catalysts supported on various metal oxides. *J. Catal.* **2016**, *343*, 178–184. [CrossRef]
111. Vita, A.; Italiano, C.; Pino, L.; Frontera, P.; Ferraro, M.; Antonucci, V. Activity and stability of powder and monolith-coated Ni/GDC catalysts for CO_2 methanation. *Appl. Catal. B Environ.* **2018**, *226*, 384–395. [CrossRef]
112. Liu, Y.; Zong, X.; Patra, A.; Caratzoulas, S.; Vlachos, D.G. Propane Dehydrogenation on PtxSny (x, y $\leq$ 4) Clusters on Al_2O_3(110). *ACS Catal.* **2023**, *13*, 2802–2812. [CrossRef]
113. Cai, M.; Wen, J.; Chu, W.; Cheng, X.; Li, Z. Methanation of carbon dioxide on Ni/ZrO_2-Al_2O_3 catalysts: Effects of ZrO_2 promoter and preparation method of novel ZrO_2-Al_2O_3 carrier. *J. Nat. Gas Chem.* **2011**, *20*, 318–324. [CrossRef]
114. Dias, Y.R.; Bernardi, F.; Perez-Lopez, O.W. Improving Low-Temperature CO_2 Methanation by Promoting Ni-Al LDH-Derived Catalysts with Alkali Metals. *ChemCatChem* **2023**, 202300834. [CrossRef]
115. Riani, P.; Garbarino, G.; Lucchini, M.A.; Canepa, F.; Busca, G. Unsupported versus alumina-supported Ni nanoparticles as catalysts for steam/ethanol conversion and CO_2 methanation. *J. Mol. Catal. A Chem.* **2014**, *383–384*, 10–16. [CrossRef]
116. Kim, M.J.; Youn, J.R.; Kim, H.J.; Seo, M.W.; Lee, D.; Go, K.S.; Lee, K.B.; Jeon, S.G. Effect of surface properties controlled by Ce addition on CO_2 methanation over Ni/Ce/Al_2O_3 catalyst. *Int. J. Hydrogen Energy* **2020**, *45*, 24595–24603. [CrossRef]
117. Liu, Y.; McGill, C.J.; Green, W.H.; Deshlahra, P. Effects of surface species and homogeneous reactions on rates and selectivity in ethane oxidation on oxide catalysts. *AIChE J.* **2021**, *67*, e17483. [CrossRef]
118. Velty, A.; Corma, A. Advanced zeolite and ordered mesoporous silica-based catalysts for the conversion of CO_2 to chemicals and fuels. *Chem. Soc. Rev.* **2023**, *52*, 1773–1946. [CrossRef] [PubMed]
119. Ye, R.P.; Ding, J.; Gong, W.; Argyle, M.D.; Zhong, Q.; Wang, Y.; Russell, C.K.; Xu, Z.; Russell, A.G.; Li, Q.; et al. CO_2 hydrogenation to high-value products via heterogeneous catalysis. *Nat. Commun.* **2019**, *10*, 5698. [CrossRef] [PubMed]
120. Liu, C.J.; Ye, J.; Jiang, J.; Pan, Y. Progresses in the preparation of coke resistant Ni-based catalyst for steam and CO_2 reforming of methane. *ChemCatChem* **2011**, *3*, 529–541. [CrossRef]
121. Li, S.; Guo, S.; Gong, D.; Kang, N.; Fang, K.G.; Liu, Y. Nano composite composed of MoO_x-La_2O_3–Ni on SiO_2 for storing hydrogen into CH_4 via CO_2 methanation. *Int. J. Hydrogen Energy* **2019**, *44*, 1597–1609. [CrossRef]
122. Ma, H.; Ma, K.; Ji, J.; Tang, S.; Liu, C.; Jiang, W.; Yue, H.; Liang, B. Graphene intercalated Ni-SiO_2/GO-Ni-foam catalyst with enhanced reactivity and heat-transfer for CO_2 methanation. *Chem. Eng. Sci.* **2019**, *194*, 10–21. [CrossRef]
123. Guo, M.; Lu, G. The difference of roles of alkaline-earth metal oxides on silica-supported nickel catalysts for CO_2 methanation. *RSC Adv.* **2014**, *4*, 58171–58177. [CrossRef]
124. Guo, M.; Lu, G. The effect of impregnation strategy on structural characters and CO_2 methanation properties over MgO modified Ni/SiO_2 catalysts. *Catal. Commun.* **2014**, *54*, 55–60. [CrossRef]
125. Gac, W.; Zawadzki, W.; Słowik, G.; Sienkiewicz, A.; Kierys, A. Nickel catalysts supported on silica microspheres for CO_2 methanation. *Microporous Mesoporous Mater.* **2018**, *272*, 79–91. [CrossRef]
126. Sokolov, S.; Kondratenko, E.V.; Pohl, M.M.; Barkschat, A.; Rodemerck, U. Stable low-temperature dry reforming of methane over mesoporous La_2O_3-ZrO_2 supported Ni catalyst. *Appl. Catal. B Environ.* **2012**, *113–114*, 19–30. [CrossRef]
127. Rossetti, I.; Biffi, C.; Bianchi, C.L.; Nichele, V.; Signoretto, M.; Menegazzo, F.; Finocchio, E.; Ramis, G.; Di Michele, A. Ni/SiO_2 and Ni/ZrO_2 catalysts for the steam reforming of ethanol. *Appl. Catal. B Environ.* **2012**, *117–118*, 384–396. [CrossRef]
128. Moghaddam, S.V.; Rezaei, M.; Meshkani, F.; Daroughegi, R. Synthesis of nanocrystalline mesoporous Ni/Al_2O_3–SiO_2 catalysts for CO_2 methanation reaction. *Int. J. Hydrogen Energy* **2018**, *43*, 19038–19046. [CrossRef]
129. Li, Y.; Lu, G.; Ma, J. Highly active and stable nano NiO-MgO catalyst encapsulated by silica with a core-shell structure for CO_2 methanation. *RSC Adv.* **2014**, *4*, 17420–17428. [CrossRef]
130. Aziz, M.A.A.; Jalil, A.A.; Triwahyono, S.; Mukti, R.R.; Taufiq-Yap, Y.H.; Sazegar, M.R. Highly active Ni-promoted mesostructured silica nanoparticles for CO_2 methanation. *Appl. Catal. B Environ.* **2014**, *147*, 359–368. [CrossRef]
131. Aziz, M.A.A.; Jalil, A.A.; Triwahyono, S.; Saad, M.W.A. CO_2 methanation over Ni-promoted mesostructured silica nanoparticles: Influence of Ni loading and water vapor on activity and response surface methodology studies. *Chem. Eng. J.* **2015**, *260*, 757–764. [CrossRef]
132. Aziz, M.A.A.; Jalil, A.A.; Triwahyono, S.; Ahmad, A. CO_2 methanation over heterogeneous catalysts: Recent progress and future prospects. *Green Chem.* **2015**, *17*, 2647–2663. [CrossRef]
133. Rahmani, S.; Rezaei, M.; Meshkani, F. Preparation of highly active nickel catalysts supported on mesoporous nanocrystalline γ-Al_2O_3 for CO_2 methanation. *J. Ind. Eng. Chem.* **2014**, *20*, 1346–1352. [CrossRef]
134. Liu, Q.; Bian, B.; Fan, J.; Yang, J. Cobalt doped Ni based ordered mesoporous catalysts for CO_2 methanation with enhanced catalytic performance. *Int. J. Hydrogen Energy* **2018**, *43*, 4893–4901. [CrossRef]
135. Gac, W.; Zawadzki, W.; Rotko, M.; Greluk, M.; Słowik, G.; Kolb, G. Effects of support composition on the performance of nickel catalysts in CO_2 methanation reaction. *Catal. Today* **2020**, *357*, 468–482. [CrossRef]
136. Li, W.; Wang, H.; Jiang, X.; Zhu, J.; Liu, Z.; Guo, X.; Song, C. A short review of recent advances in CO_2 hydrogenation to hydrocarbons over heterogeneous catalysts. *RSC Adv.* **2018**, *8*, 7651–7669. [CrossRef] [PubMed]

137. Lin, J.; Ma, C.; Wang, Q.; Xu, Y.; Ma, G.; Wang, J.; Wang, H.; Dong, C.; Zhang, C.; Ding, M. Enhanced low-temperature performance of CO_2 methanation over mesoporous Ni/Al_2O_3-ZrO_2 catalysts. *Appl. Catal. B Environ.* **2019**, *243*, 262–272. [CrossRef]
138. Zhao, K.; Li, Z.; Bian, L. CO_2 methanation and co-methanation of CO and CO_2 over Mn-promoted Ni/Al_2O_3 catalysts. *Front. Chem. Sci. Eng.* **2016**, *10*, 273–280. [CrossRef]
139. Ahmad, W.; Younis, M.N.; Shawabkeh, R.; Ahmed, S. Synthesis of lanthanide series (La, Ce, Pr, Eu & Gd) promoted Ni/Γ-Al_2O_3 catalysts for methanation of CO_2 at low temperature under atmospheric pressure. *Catal. Commun.* **2017**, *100*, 121–126. [CrossRef]
140. Müller, K.; Fleige, M.; Rachow, F.; Schmeißer, D. Sabatier based CO_2-methanation of flue gas emitted by conventional power plants. *Energy Procedia* **2013**, *40*, 240–248. [CrossRef]
141. Gong, D.; Li, S.; Guo, S.; Tang, H.; Wang, H.; Liu, Y. Lanthanum and cerium co-modified Ni/SiO_2 catalyst for CO methanation from syngas. *Appl. Surf. Sci.* **2018**, *434*, 351–364. [CrossRef]
142. Zhen, W.; Li, B.; Lu, G.; Ma, J. Enhancing catalytic activity and stability for CO_2 methanation on Ni@MOF-5 via control of active species dispersion. *Chem. Commun.* **2015**, *51*, 1728–1731. [CrossRef] [PubMed]
143. Chen, Y.; Qiu, B.; Liu, Y.; Zhang, Y. An active and stable nickel-based catalyst with embedment structure for CO_2 methanation. *Appl. Catal. B Environ.* **2020**, *269*, 118801. [CrossRef]
144. Aljishi, A.; Veilleux, G.; Lalinde, J.A.H.; Kopyscinski, J. The effect of synthesis parameters on ordered mesoporous nickel alumina catalyst for CO_2 methanation. *Appl. Catal. A Gen.* **2018**, *549*, 263–272. [CrossRef]
145. Wang, W.; Chu, W.; Wang, N.; Yang, W.; Jiang, C. Mesoporous nickel catalyst supported on multi-walled carbon nanotubes for carbon dioxide methanation. *Int. J. Hydrogen Energy* **2016**, *41*, 967–975. [CrossRef]
146. Dong, H.; Liu, Q. Three-Dimensional Networked Ni-Phyllosilicate Catalyst for CO_2 Methanation: Achieving High Dispersion and Enhanced Stability at High Ni Loadings. *ACS Sustain. Chem. Eng.* **2020**, *8*, 6753–6766. [CrossRef]
147. Summa, P.; Samojeden, B.; Motak, M.; Wierzbicki, D.; Alxneit, I.; Świerczek, K.; Da Costa, P. Investigation of Cu promotion effect on hydrotalcite-based nickel catalyst for CO_2 methanation. *Catal. Today* **2022**, *384–386*, 133–145. [CrossRef]
148. Sun, C.; Świrk Da Costa, K.; Wang, Y.; Scheidl, K.S.; Breiby, D.W.; Rønning, M.; Hu, C.; Da Costa, P. Tailoring the yttrium content in Ni-Ce-Y/SBA-15 mesoporous silicas for CO_2 methanation. *Catal. Today* **2021**, *382*, 104–119. [CrossRef]
149. Bacariza, M.C.; Graça, I.; Bebiano, S.S.; Lopes, J.M.; Henriques, C. Magnesium as Promoter of CO_2 Methanation on Ni-Based USY Zeolites. *Energy and Fuels* **2017**, *31*, 9776–9789. [CrossRef]
150. Jiang, Y.; Huang, T.; Dong, L.; Su, T.; Li, B.; Luo, X.; Xie, X.; Qin, Z.; Xu, C.; Ji, H. Mn modified Ni/bentonite for CO_2 methanation. *Catalysts* **2018**, *8*, 646. [CrossRef]
151. Zhang, L.; Bian, L.; Zhu, Z.; Li, Z. La-promoted Ni/Mg-Al catalysts with highly enhanced low-temperature CO_2 methanation performance. *Int. J. Hydrogen Energy* **2018**, *43*, 2197–2206. [CrossRef]
152. Garbarino, G.; Wang, C.; Cavattoni, T.; Finocchio, E.; Riani, P.; Flytzani-Stephanopoulos, M.; Busca, G. A study of Ni/La-Al_2O_3 catalysts: A competitive system for CO_2 methanation. *Appl. Catal. B Environ.* **2019**, *248*, 286–297. [CrossRef]
153. Liu, J.; Li, C.; Wang, F.; He, S.; Chen, H.; Zhao, Y.; Wei, M.; Evans, D.G.; Duan, X. Enhanced low-temperature activity of CO_2 methanation over highly-dispersed Ni/TiO_2 catalyst. *Catal. Sci. Technol.* **2013**, *3*, 2627–2633. [CrossRef]
154. Zhao, K.; Wang, W.; Li, Z. Highly efficient Ni/ZrO_2 catalysts prepared via combustion method for CO_2 methanation. *J. CO2 Util.* **2016**, *16*, 236–244. [CrossRef]
155. Ye, R.P.; Li, Q.; Gong, W.; Wang, T.; Razink, J.J.; Lin, L.; Qin, Y.Y.; Zhou, Z.; Adidharma, H.; Tang, J.; et al. *High-Performance of Nanostructured Ni/CeO_2 Catalyst on CO_2 Methanation*; Elsevier B.V.: Amsterdam, The Netherlands, 2020; Volume 268, ISBN 0000000175.
156. Ocampo, F.; Louis, B.; Roger, A.C. Methanation of carbon dioxide over nickel-based $Ce_{0.72}Zr_{0.28}O_2$ mixed oxide catalysts prepared by sol-gel method. *Appl. Catal. A Gen.* **2009**, *369*, 90–96. [CrossRef]
157. Ashok, J.; Ang, M.L.; Kawi, S. Enhanced activity of CO_2 methanation over Ni/CeO_2-ZrO_2 catalysts: Influence of preparation methods. *Catal. Today* **2017**, *281*, 304–311. [CrossRef]
158. Vrijburg, W.L.; Van Helden, J.W.A.; Parastaev, A.; Groeneveld, E.; Pidko, E.A.; Hensen, E.J.M. Ceria-zirconia encapsulated Ni nanoparticles for CO_2 methanation. *Catal. Sci. Technol.* **2019**, *9*, 5001–5010. [CrossRef]
159. Pastor-Pérez, L.; Le Saché, E.; Jones, C.; Gu, S.; Arellano-Garcia, H.; Reina, T.R. Synthetic natural gas production from CO_2 over Ni-x/CeO_2-ZrO_2 (x = Fe, Co) catalysts: Influence of promoters and space velocity. *Catal. Today* **2018**, *317*, 108–113. [CrossRef]
160. Atzori, L.; Rombi, E.; Meloni, D.; Sini, M.F.; Monaci, R.; Cutrufello, M.G. CO and CO_2 Co-Methanation on Ni/CeO_2-ZrO_2 Soft-Templated Catalysts. *Catalysts* **2019**, *9*, 415. [CrossRef]
161. Li, S.; Liu, G.; Zhang, S.; An, K.; Ma, Z.; Wang, L.; Liu, Y. Cerium-modified Ni-La_2O_3/ZrO_2 for CO_2 methanation. *J. Energy Chem.* **2020**, *43*, 155–164. [CrossRef]
162. Liu, H.; Zou, X.; Wang, X.; Lu, X.; Ding, W. Effect of CeO_2 addition on Ni/Al_2O_3 catalysts for methanation of carbon dioxide with hydrogen. *J. Nat. Gas Chem.* **2012**, *21*, 703–707. [CrossRef]
163. Schubert, M.; Pokhrel, S.; Thomé, A.; Zielasek, V.; Gesing, T.M.; Roessner, F.; Mädler, L.; Bäumer, M. Highly active Co-Al_2O_3-based catalysts for CO_2 methanation with very low platinum promotion prepared by double flame spray pyrolysis. *Catal. Sci. Technol.* **2016**, *6*, 7449–7460. [CrossRef]
164. Alrafei, B.; Polaert, I.; Ledoux, A.; Azzolina-Jury, F. Remarkably stable and efficient Ni and Ni-Co catalysts for CO_2 methanation. *Catal. Today* **2020**, *346*, 23–33. [CrossRef]

165. Chen, H.; Fu, J.; Zhang, P.; Peng, H.; Abney, C.W.; Jie, K.; Liu, X.; Chi, M.; Dai, S. Entropy-stabilized metal oxide solid solutions as CO oxidation catalysts with high-temperature stability. *J. Mater. Chem. A* **2018**, *6*, 11129–11133. [CrossRef]
166. Liu, X.; Wang, X.; Sun, H.; Zhang, Z.; Song, P.; Liu, Y. Highly Stable Bimetal Ni-Co on Alumina-Covered Spinel Oxide Derived from High Entropy Oxide for CO_2 Methanation. *Ind. Eng. Chem. Res.* **2023**, *62*, 341–354. [CrossRef]
167. Jimenez, J.D.; Wen, C.; Lauterbach, J. Design of highly active cobalt catalysts for CO_2 hydrogenation: Via the tailoring of surface orientation of nanostructures. *Catal. Sci. Technol.* **2019**, *9*, 1970–1978. [CrossRef]
168. Jimenez, J.; Bird, A.; Santos Santiago, M.; Wen, C.; Lauterbach, J. Supported Cobalt Nanorod Catalysts for Carbon Dioxide Hydrogenation. *Energy Technol.* **2017**, *5*, 884–891. [CrossRef]
169. Liang, L.; Miao, C.; Chen, S.; Zheng, X.; Ouyang, J. Effective CO_2 methanation at ambient pressure over Lanthanides (La/Ce/Pr/Sm) modified cobalt-palygorskite composites. *J. CO2 Util.* **2022**, *63*, 102114. [CrossRef]
170. Li, W.; Nie, X.; Jiang, X.; Zhang, A.; Ding, F.; Liu, M.; Liu, Z.; Guo, X.; Song, C. ZrO_2 support imparts superior activity and stability of Co catalysts for CO_2 methanation. *Appl. Catal. B Environ.* **2018**, *220*, 397–408. [CrossRef]
171. Li, W.; Liu, Y.; Mu, M.; Ding, F.; Liu, Z.; Guo, X.; Song, C. Organic acid-assisted preparation of highly dispersed Co/ZrO_2 catalysts with superior activity for CO_2 methanation. *Appl. Catal. B Environ.* **2019**, *254*, 531–540. [CrossRef]
172. Tu, J.; Wu, H.; Qian, Q.; Han, S.; Chu, M.; Jia, S.; Feng, R.; Zhai, J.; He, M.; Han, B. Low temperature methanation of CO_2 over an amorphous cobalt-based catalyst. *Chem. Sci.* **2021**, *12*, 3937–3943. [CrossRef]
173. Valinejad Moghaddam, S.; Rezaei, M.; Meshkani, F.; Daroughegi, R. Carbon dioxide methanation over Ni-M/Al_2O_3 (M: Fe, CO, Zr, La and Cu) catalysts synthesized using the one-pot sol-gel synthesis method. *Int. J. Hydrogen Energy* **2018**, *43*, 16522–16533. [CrossRef]
174. Yin, L.; Chen, X.; Sun, M.; Zhao, B.; Chen, J.; Zhang, Q.; Ning, P. Insight into the role of Fe on catalytic performance over the hydrotalcite-derived Ni-based catalysts for CO_2 methanation reaction. *Int. J. Hydrogen Energy* **2022**, *47*, 7139–7149. [CrossRef]
175. Lan, P.W.; Wang, C.C.; Chen, C.Y. Effect of Ni/Fe ratio in Ni–Fe catalysts prepared under external magnetic field on CO_2 methanation. *J. Taiwan Inst. Chem. Eng.* **2021**, *127*, 166–174. [CrossRef]
176. Everett, O.E.; Zonetti, P.C.; Alves, O.C.; de Avillez, R.R.; Appel, L.G. The role of oxygen vacancies in the CO_2 methanation employing Ni/ZrO_2 doped with Ca. *Int. J. Hydrogen Energy* **2020**, *45*, 6352–6359. [CrossRef]
177. Yamasaki, M.; Habazaki, H.; Yoshida, T.; Akiyama, E.; Kawashima, A.; Asami, K.; Hashimoto, K.; Komori, M.; Shimamura, K. Compositional dependence of the CO_2 methanation activity of Ni/ZrO_2 catalysts prepared from amorphous Ni-Zr alloy precursors. *Appl. Catal. A Gen.* **1997**, *163*, 187–197. [CrossRef]
178. Tan, J.; Wang, J.; Zhang, Z.; Ma, Z.; Wang, L.; Liu, Y. Highly dispersed and stable Ni nanoparticles confined by MgO on ZrO_2 for CO_2 methanation. *Appl. Surf. Sci.* **2019**, *481*, 1538–1548. [CrossRef]
179. Ren, J.; Qin, X.; Yang, J.Z.; Qin, Z.F.; Guo, H.L.; Lin, J.Y.; Li, Z. Methanation of carbon dioxide over Ni-M/ZrO_2 (M = Fe, Co, Cu) catalysts: Effect of addition of a second metal. *Fuel Process. Technol.* **2015**, *137*, 204–211. [CrossRef]
180. Tian, J.; Zheng, P.; Zhang, T.; Han, Z.; Xu, W.; Gu, F.; Wang, F.; Zhang, Z.; Zhong, Z.; Su, F.; et al. CO_2 methanation over Ni nanoparticles inversely loaded with CeO_2 and Cr_2O_3: Catalytic functions of metal oxide/Ni interfaces. *Appl. Catal. B Environ.* **2023**, *339*, 123121. [CrossRef]
181. Qin, Z.; Ren, J.; Miao, M.; Li, Z.; Lin, J.; Xie, K. The catalytic methanation of coke oven gas over Ni-Ce/Al_2O_3 catalysts prepared by microwave heating: Effect of amorphous NiO formation. *Appl. Catal. B Environ.* **2015**, *164*, 18–30. [CrossRef]
182. Konishcheva, M.V.; Potemkin, D.I.; Badmaev, S.D.; Snytnikov, P.V.; Paukshtis, E.A.; Sobyanin, V.A.; Parmon, V.N. On the Mechanism of CO and CO_2 Methanation Over Ni/CeO_2 Catalysts. *Top. Catal.* **2016**, *59*, 1424–1430. [CrossRef]
183. Nematollahi, B.; Rezaei, M.; Lay, E.N. Selective methanation of carbon monoxide in hydrogen rich stream over Ni/CeO_2 nanocatalysts. *J. Rare Earths* **2015**, *33*, 619–628. [CrossRef]
184. Laosiripojana, N.; Assabumrungrat, S. Methane steam reforming over Ni/Ce-ZrO_2 catalyst: Influences of Ce-ZrO_2 support on reactivity, resistance toward carbon formation, and intrinsic reaction kinetics. *Appl. Catal. A Gen.* **2005**, *290*, 200–211. [CrossRef]
185. Di Monte, R.; Fornasiero, P.; Kašpar, J.; Rumori, P.; Gubitosa, G.; Graziani, M. Pd/$Ce_{0.6}Zr_{0.4}O_2$/Al_2O_3 as advanced materials for three-way catalysts. Part 1. Catalyst characterisation, thermal stability and catalytic activity in the reduction of NO by CO. *Appl. Catal. B Environ.* **2000**, *24*, 157–167. [CrossRef]
186. Strobel, R.; Krumeich, F.; Pratsinis, S.E.; Baiker, A. Flame-derived Pt/Ba/$Ce_xZr_{1-x}O_2$: Influence of support on thermal deterioration and behavior as NO_x storage-reduction catalysts. *J. Catal.* **2006**, *243*, 229–238. [CrossRef]
187. Le, T.A.; Kim, M.S.; Lee, S.H.; Park, E.D. CO and CO_2 Methanation Over Supported Cobalt Catalysts. *Top. Catal.* **2017**, *60*, 714–720. [CrossRef]
188. Youn, M.H.; Seo, J.G.; Cho, K.M.; Park, S.; Park, D.R.; Jung, J.C.; Song, I.K. Hydrogen production by auto-thermal reforming of ethanol over nickel catalysts supported on Ce-modified mesoporous zirconia: Effect of Ce/Zr molar ratio. *Int. J. Hydrogen Energy* **2008**, *33*, 5052–5059. [CrossRef]
189. Silva, P.P.; Silva, F.A.; Portela, L.S.; Mattos, L.V.; Noronha, F.B.; Hori, C.E. Effect of Ce/Zr ratio on the performance of Pt/$CeZrO_2$/Al_2O_3 catalysts for methane partial oxidation. *Catal. Today* **2005**, *107–108*, 734–740. [CrossRef]
190. Koubaissy, B.; Pietraszek, A.; Roger, A.C.; Kiennemann, A. CO_2 reforming of methane over Ce-Zr-Ni-Me mixed catalysts. *Catal. Today* **2010**, *157*, 436–439. [CrossRef]
191. ten Have, I.C.; Kromwijk, J.J.G.; Monai, M.; Ferri, D.; Sterk, E.B.; Meirer, F.; Weckhuysen, B.M. Uncovering the reaction mechanism behind CoO as active phase for CO_2 hydrogenation. *Nat. Commun.* **2022**, *13*. [CrossRef]

192. Visconti, C.G.; Martinelli, M.; Falbo, L.; Fratalocchi, L.; Lietti, L. CO_2 hydrogenation to hydrocarbons over Co and Fe-based Fischer-Tropsch catalysts. *Catal. Today* **2016**, *277*, 161–170. [CrossRef]
193. Jimenez, J.D.; Wen, C.; Royko, M.M.; Kropf, A.J.; Segre, C.; Lauterbach, J. Influence of Coordination Environment of Anchored Single-Site Cobalt Catalyst on CO_2 Hydrogenation. *ChemCatChem* **2020**, *12*, 846–854. [CrossRef]
194. Zhang, Y.; Jacobs, G.; Sparks, D.E.; Dry, M.E.; Davis, B.H. CO and CO_2 hydrogenation study on supported cobalt Fischer-Tropsch synthesis catalysts. *Catal. Today* **2002**, *71*, 411–418. [CrossRef]
195. Ishchenko, O.V.; Dyachenko, A.G.; Yatsymyrskiy, A.V.; Zakharova, T.M.; Gaidai, S.V.; Lisnyak, V.V.; Mariychuk, R. CO_2 methanation over Co-Ni catalysts. *E3S Web Conf.* **2020**, *154*, 02001. [CrossRef]
196. Huynh, H.L.; Zhu, J.; Zhang, G.; Shen, Y.; Tucho, W.M.; Ding, Y.; Yu, Z. Promoting effect of Fe on supported Ni catalysts in CO_2 methanation by in situ DRIFTS and DFT study. *J. Catal.* **2020**, *392*, 266–277. [CrossRef]